CHAPTER 3

SYNTHESIS OF HIGHER MOLECULAR WEIGHT POLY(GLYCOLIC ACID)

3.1 Previous Work [17, 20, 31-33, 43-48]

The direct polyesterification of glycolic acid, according to the method previously described in Chapter 2, gives only low molecular weight poly(glycolic acid). The preparation of high molecular weight polymers of glycolic acid is extremely difficult using conventional condensation techniques due to the stepwise nature of the condensation reaction.

Since the pioneering work of Carothers [1], cyclic diesters and their alkyl- and aryl-substituted derivatives have been known to be suitable starting materials for the preparation of linear aliphatic poly-α-esters. Hence, for most applications, it is preferable to prepare the polymer using the cyclic dimer as the starting material. This method is advantageous because higher molecular weight polymers may be obtained without carrying the reaction to such a high degree of completion. Some problems associated with the polymerisation of linear monomers at high temperature, such as by-product removal, exact

stoichiometry and side reactions, may be avoided in the polymerisation of cyclic esters.

Many kinds of catalysts have been used to initiate the ring-opening polymerisation of cyclic esters. These include compounds of cadmium, tin, lead, titanium, zinc, antimony, and a variety of amines. For intermediate molecular weights (10,000 - 40,000) [32], acid-catalysed bulk polymerisation is convenient and effective.

The cyclic dimer of glycolic acid is glycolide which is prepared by a two-step process as shown below.

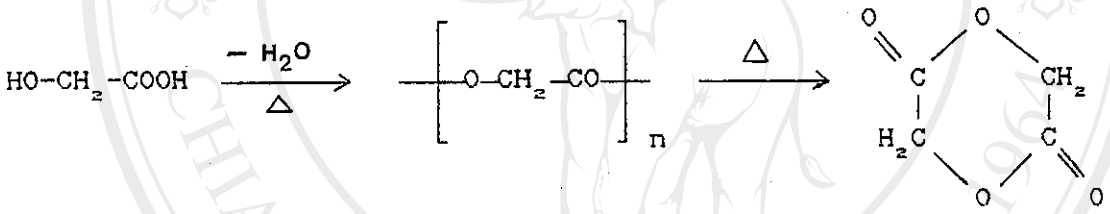

glycolic acid low molecular weight PGA glycolide

It is generally understood that the glycolide is not formed directly from the bimolecular cyclization of glycolic acid; instead, it is formed indirectly from the thermal decomposition of low molecular weight poly(glycolic acid). This thermal decomposition occurs via an intramolecular ester interchange mechanism, as will be described in more detail later. The crude glycolide is then purified and finally polymerised in bulk by ring-opening polymerisation to high molecular weight PGA.

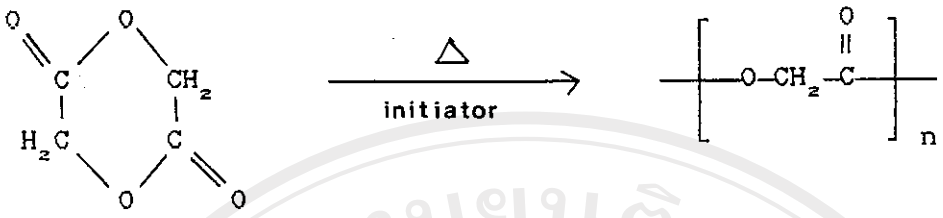

high molecular weight PGA

3.2 Synthesis of Glycolide [3, 23, 32-33, 45]

The experimental procedure followed was based on the methods given in earlier literature reports [32-33]. Also, reference was made to the kinetic studies in Chapter 2 in which the low molecular weight poly(glycolic acid) precursor was obtained under various reaction conditions. Based on these considerations, a total of 3 experiments were designed :

(1) RUN 1 : Uncatalysed polyesterification followed by Sb_2O_3-catalysed thermal decomposition

(2) RUN 2 : PTSA-catalysed polyesterification followed by Sb_2O_3-catalysed thermal decomposition

(3) RUN 3 : Sb_2O_3-catalysed polyesterification followed by Sb_2O_3-catalysed thermal decomposition

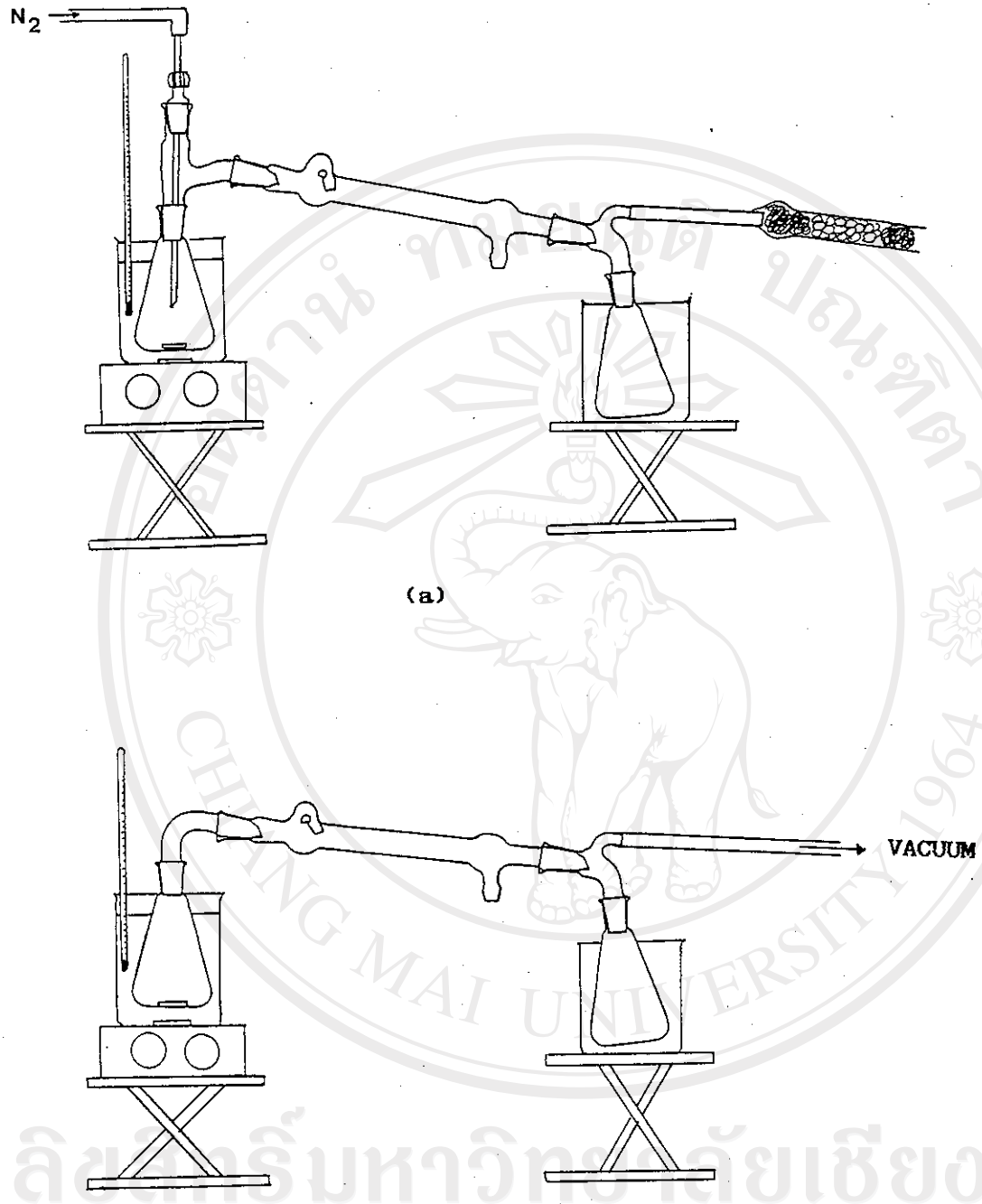

Fig. 3.1 : Apparatus used in the two-stage preparation of glycolide :

(a) glycolic acid polycondensation to low mol. wt. PGA;

(b) thermal degradation of low mol. wt. PGA to glycolide.

3.2.1 RUN 1 : Uncatalysed Polyesterification followed by Antimony Trioxide-Catalysed Thermal Decomposition

Approximately 50 g of glycolic acid were heated at 150 °C under an atmospheric pressure of nitrogen gas in a conventional short-path distillation apparatus (see Fig. 3.1 a). Heating was continued for 3 hours until the water of polycondensation ceased to distill from the flask. The apparatus was then adapted for vacuum take-off (see Fig. 3.1 b) and heated at 180 °C under a reduced pressure of about 2-4 mm Hg. Heating was continued for about 3 hours. At the end of this period, the residue in the heating flask was allowed to cool to room temprature. This intermediate product was low molecular weight poly(glycolic acid) and was obtained as a white solid substance. Its number-average molecular weight, $\overline{M}_n$, was determined by end-group analysis of a small sample of the product.

Then, 0.50 g of antimony trioxide was added to the flask as degradation catalyst and the mixture heated up to about 285 °C under a reduced pressure of about 2-4 mm Hg for an additional period of about 4-5 hours. When the temperature reached about 230 °C, the low molecular weight PGA completely melted; continued heating to about 240-250 °C then caused the residue in the heating flask to darken in colour until it eventually turned black. Continued heating up to 285 °C yielded glycolide as the primary degradation product. Crude glycolide began to distill out of the flask and solidify in the condenser at about 260-270 °C. Heating was continued until distillation ceased. This crude product was obtained as a crystalline solid with a slight greenish-yellow discoloration.

The crude glycolide product which had collected in the condenser was carefully and quickly removed due to its hygroscopic nature. It was then quickly ground up and purified by recrystallisation from distilled ethyl acetate, the crystallised material being a white crystalline solid of melting point 82-84 °C (lit. [32] m.p. 82-84 °C). The results of this RUN 1 glycolide synthesis are summarized in Table 3.1.

3.2.2 RUN 2 : p-Toluenesulfonic Acid-Catalysed Polyesterification followed by Antimony Trioxide-Catalysed Thermal Decomposition

For RUN 2, approximately 0.50 g of PTSA catalyst (1% w/w) were added to the approximately 50 g of glycolic acid in the heating flask. Apart from this, the method and conditions used corresponded to these previously described in RUN 1.

The crude glycolide product obtained was a crystalline solid with a slight orange-brown discoloration. After purification by recrystallisation from distilled ethyl acetate, the pure material was a white crystalline solid which appeared to be combined with a minor amount of a pale cream-coloured powder. The observed melting point of the pure glycolide was 80-82 °C. The results of this RUN 2 synthesis are also summarized in Table 3.1.

3.2.3 RUN 3 : Antimony Trioxide-Catalysed Polyesterification followed by Antimony Trioxide-Catalysed Thermal Decomposition

For RUN 3, approximately 0.5 g of antimony trioxide (Sb_2O_3) catalyst (1% w/w) were added to approximately 50 g of glycolic acid in the heating flask and heated under the same conditions as in RUN 1 to produce low molecular weight PGA. Since the same 0.5 g Sb_2O_3 was the catalyst for both the polyesterification and thermal degradation steps, intermediate cooling was not necessary before the temperature was increased up to 285 °C under reduced pressure. The observed changes in the reaction mixture were similar to those previously described for RUN 1.

The crude glycolide was obtained as a slightly greenish-yellow coloured crystalline solid which collected in the condenser. After recrystallisation from distilled ethyl acetate, the pure glycolide product was a white crystalline solid of melting point 82-84 °C. The results of this RUN 3 systhesis are compared alongside those of RUNS 1 and 2 in Table 3.1.

Table 3.1 : The synthesis of glycolide : comparison of results of RUNS 1-3.

Results Obtained	RUN 1	RUN 2	RUN 3
	Uncatalysed/Sb_2O_3	PTSA/Sb_2O_3	Sb_2O_3/Sb_2O_3
Extent of reaction, p	0.790	0.927	0.920
LOW MOL. WT. PGA			
Average degree of polymerisation, $\overline{DP}$	5	14	13
Number-average molecular weight, $\overline{M}_n$	310	830	770
CRUDE GLYCOLIDE			
- yield based on PGA	91.3 %	83.4 %	85.3 %
- yield based on GA	89.6 %	77.8 %	86.5 %
- melting point	72-80 °C	72-75 °C	72-81 °C
PURE GLYCOLIDE			
- yield based on PGA	50.7 %	38.6 %	67.7 %
- yield based on GA	49.7 %	36.0 %	68.7 %
- yield based on crude glycolide	55.5 %	46.3 %	79.4 %
- melting point	82-84 °C	80-82 °C	82-84 °C

ABBREVIATIONS :

PTSA = p-toluenesulfonic acid
PGA = poly(glycolic acid)
GA = glycolic acid

3.2.4 Structural Analysis of Glycolide by Infrared Specturometry

Fig. 3.2 shows a typical infrared (IR) spectrum of the recrystallised glycolide product. This can be compared with that in Fig. 3.3 obtained from a commercial glycolide sample (m.p. 79-82 °C, purity 99.26% , Polysciences, Inc., USA). Peak wavenumbers are compared in Table 3.2. Both spectra were obtained with the samples prepared in the form of KBr discs.

The chemical structure of glycolide is :

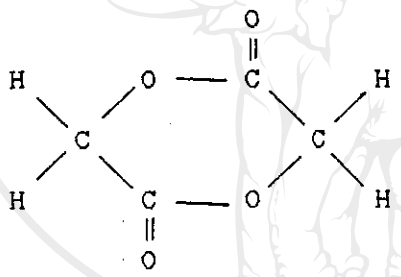

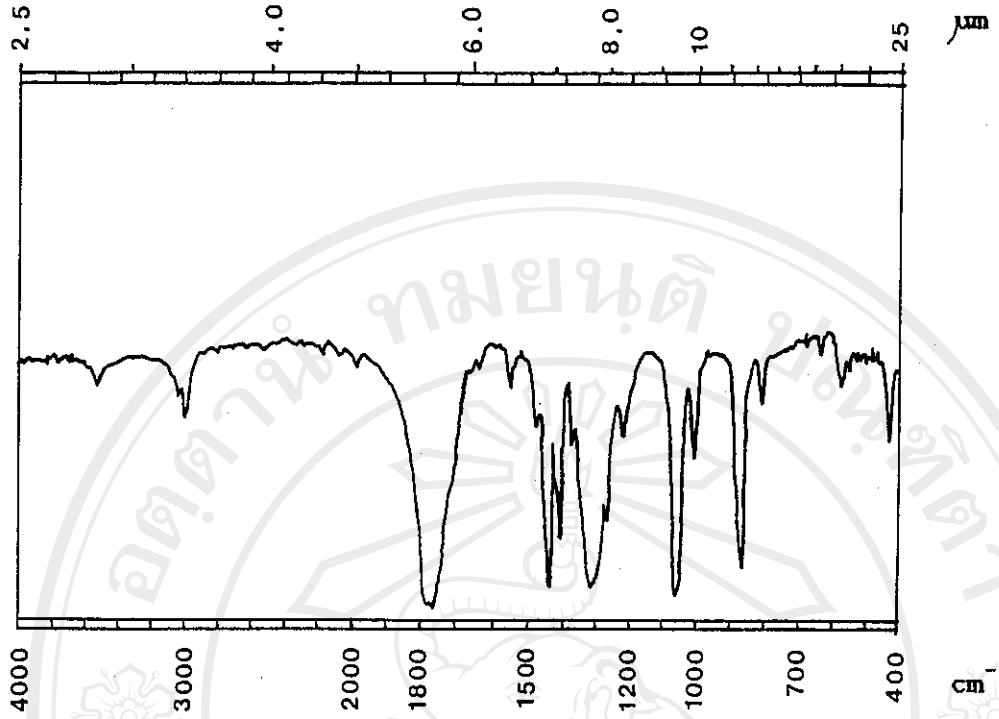

Fig. 3.2 : Infrared spectrum of recrystallised glycolide product (RUN 3).

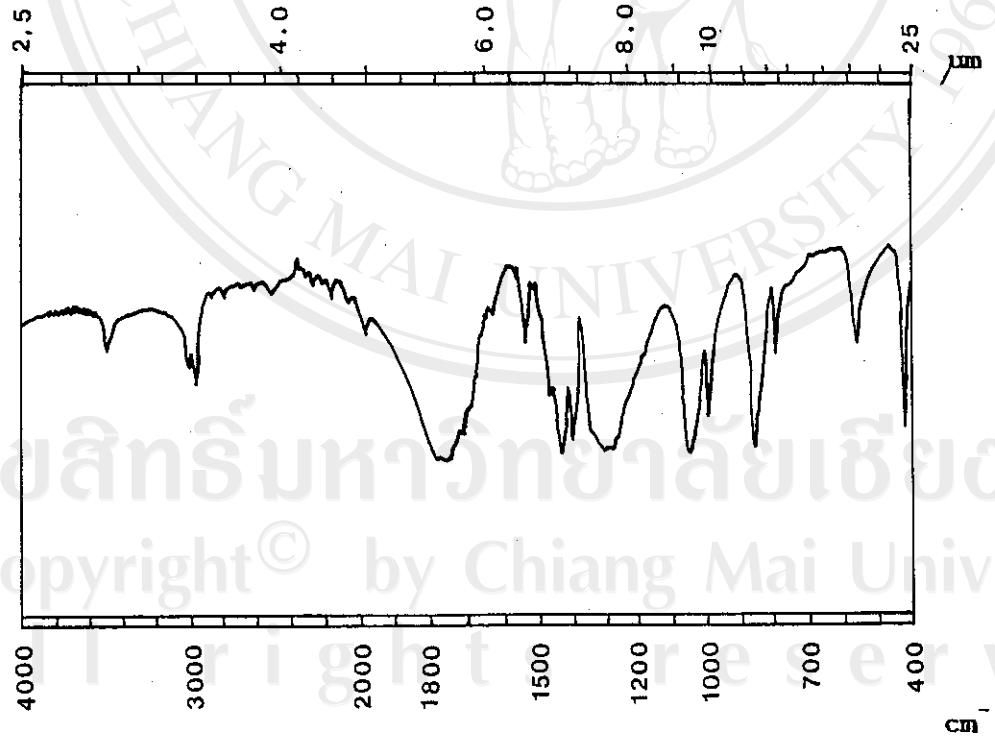

Fig. 3.3 : Infrared spectrum of commercial glycolide sample (Polysciences, Inc.).

Table 3.2 : Comparison of the infrared spectra of a recrystallised glycolide product (from RUN 3) and a commercial (Polysciences, Inc.) sample.

Vibrational Assignments	Peak Wavenumbers (cm^{-1})	
	Recrystallised Product	Commercial Sample
O-H str. (H_2O impurity)	3600 - 3450	3550 - 3400
C-H str. in CH_2	3050 - 2970	3020 - 2950
C=O str.	1800 - 1740	1860 - 1680
C-H bend.	1440, 1410, 870	1430, 1400, 860
C-O str.	1340 - 1280 (a)	1360 - 1240 (a)
	1060 (b)	1060 - 1040 (b)

NOTES :

a = in acyl-oxygen bonds (i.e., $-\overset{\overset{O}{\|}}{C}-O-$)

b = in alkyl-oxygen bonds (i.e., $-\overset{\overset{H}{|}}{\underset{\underset{H}{|}}{C}}-O-$)

str. = stretching

bend. = bending

The most prominent peaks in the IR spectra are consistent with the chemical structure of glycolide. When compared with the IR spectrum of the intermediate low molecular weight poly(glycolic acid) product (see Fig. 2.15 on page 88), the most notable differences in the glycolide spectra are those associated with :

(1) the virtual disappearance of the residual chain-end O-H stretching peaks at 3700 - 3450 cm^{-1} (in -OH and -COOH, overlapping) upon conversion to the cyclic diester; the small peak in the glycolide spectra at 3600 - 3450 cm^{-1} is probably due to absorption of atmospheric moisture since glycolide is very hygroscopic in nature;

(2) the shift of the C=O stretching peak in the glycolide spectrum to a higher wavenumber (centred at 1770 cm^{-1}) compared with that in the spectrum of the polymer precursor (centred at 1760 cm^{-1}); this is undoubtedly due to the effect of ring strain in the glycolide molecule.

3.2.5 Discussion of Glycolide Synthesis [1, 12, 23, 31-33, 45, 49-54]

The synthesis of glycolide is a two-step synthesis involving, firstly, the linear polycondensation of glycolic acid to low molecular weight PGA followed, secondly, by thermal decomposition of the PGA to yield glycolide as the primary decomposition product. The mechanism of the first step was described in the previous Chapter 2. Here, the mechanism of the second step is now described.

It was Carothers [1] who first showed that many aliphatic polyesters undergo fairly simple intramolecular ester interchange reactions producing dimeric and monomeric cyclic esters on thermal degradation. However, this was later found to apply only to those polymers capable of yielding cyclic monomers consisting of 5- to 8-membered rings. It is therefore the reverse reaction of ring-opening polymerisation. More recent studies [31] have confirmed that this type of ring-forming process is an important mechanism in the thermal degradation of poly-α-esters. Thus, poly(glycolic acid) was shown to degrade to form glycolide via an intramolecular ester interchange process [31]. Of the possible ester interchange processes, only the intramolecular exchange gave the required first-order kinetic behavior coupled with glycolide formation. It was therefore concluded that intramolecular ester interchange provided the most accurate description of the degradation process.

This mechanism for the case of poly(glycolic acid) is presented in Scheme 3.1. It explains the formation of glycolide by the type of dipolar process which is likely to be favored over the temperature range studied. Furthermore, a large and negative entropy of activation is found for PGA decomposition together with a low value for both the frequency factor and activation energy. The magnitudes of these parameters are indicative of a degradation process involving a fairly high degree of steric order in the transition state of the rate-controlling step [15]. This, again, is consistent with the mechanism shown in Scheme 3.1 with its highly ordered folded chain stereochemistry as a prelude to glycolide elimination.

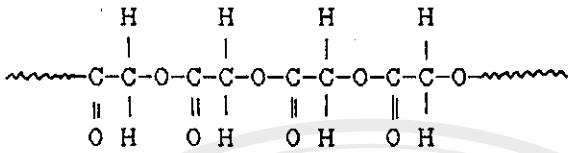

low molecular weight poly(glycolic acid)

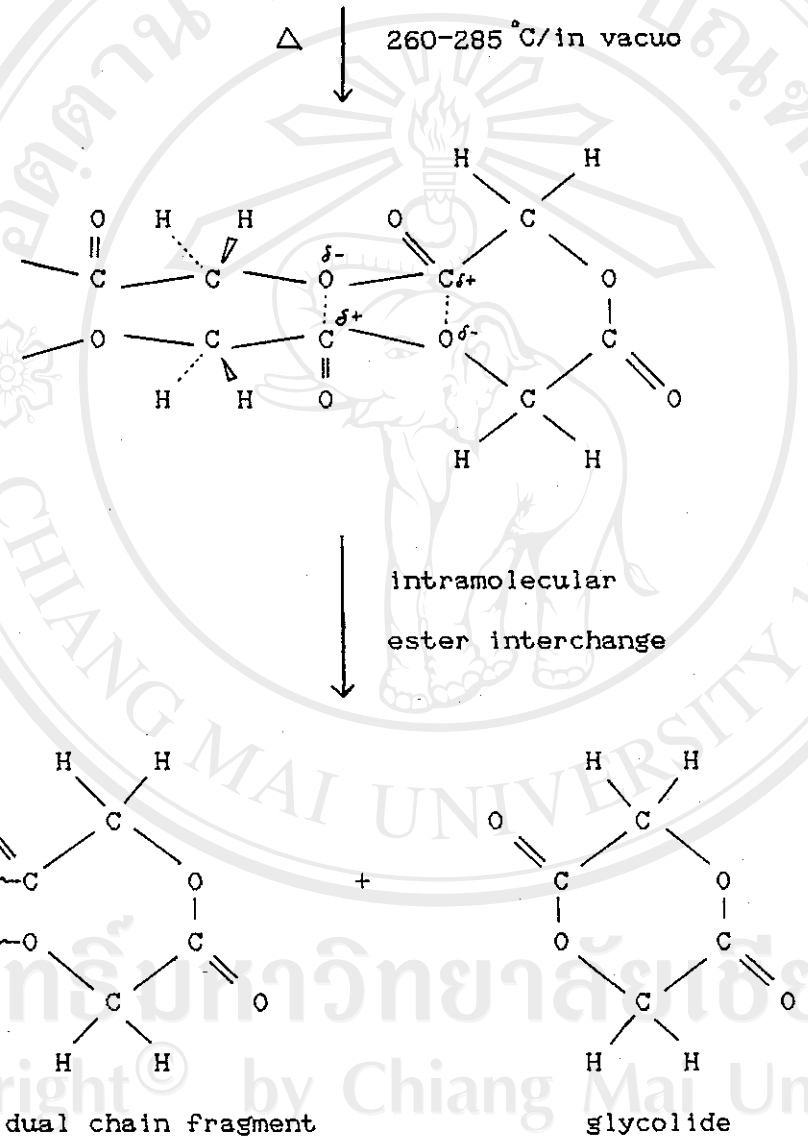

Scheme 3.1 : Mechanism of thermal degradation of poly(glycolic acid) to glycolide via intramolecular ester interchange.

In this work, three sets of conditions were compared for the synthesis of glycolide, as summarized below.

RUN 1	1st Step	Uncatalysed
	2nd Step	Sb_2O_3-catalysed
RUN 2	1st Step	PTSA-catalysed
	2nd Step	Sb_2O_3-catalysed
RUN 3	1st Step	Sb_2O_3-catalysed
	2nd Step	Sb_2O_3-catalysed

The conditions used for the 1st step polyesterifications were identical to those studied kinetically in the previous Chapter 2. For the 2nd step thermal decompositions, antimony trioxide (Sb_2O_3) was chosen as the catalyst on the basis that it is by far the most commonly used catalyst for this purpose, as reported in the literature [3, 23]. However, the actual mechanism by which Sb_2O_3 catalyses the intramolecular ester interchange process is not explained in the literature reports.

From the results obtained in this work, as summarized previously in Table 3.1, the following conclusions can be drawn :

(1) Crude glycolide was obtained in high yield (> 75%, based on the initial glycolic acid, GA) from each of the 3 RUNS. There does not appear to be any discernable dependency on the molecular weight of the intermediate PGA.

(2) The main difference between the purified glycolide products from RUNS 1, 2 and 3 was that RUNS 1 and 3 yielded what appeared to be more homogeneous crystals. The RUN 2 product seemed to be a mixture of crystals and powder. It was also found that the crude RUN 2 product could not completely dissolve in hot ethyl acetate during recrystallisation; hence the much reduced final yield (36%) of pure glycolide based on GA. A possible explanation for this may be that the glycolide from RUN 2 contained different crystal forms; glycolide has been reported in the literature [31] as being polymorphic.

(3) On comparing RUNS 1 and 3, the crude glycolide products were very similar, both in terms of yield and appearance. However, it was found that the RUN 3 product could be recrystallised in much higher yield, giving a final yield of 68.7% based on the initial GA (cf., 49.7% for RUN 1). Consequently, the conditions used in RUN 3 were considered to be the best conditions used in this work for the synthesis of glycolide. They were also the most convenient, since the antimony trioxide (Sb_2O_3) added initially acted as dual catalyst for both the polyesterification and thermal degradation steps.

Pure glycolide was generally obtained as a white crystalline solid of melting point 82-84 °C (lit. [32] m.pt. = 82-84 °C). Because of its affinity for moisture and ease of hydrolysis, the recrystallised material needed to be stored under vacuum in a vacuum desiccator at room temperature until required for use. Even under these conditions, it was found that samples of both crude and pure glycolide tended to exhibit significant changes in their melting ranges after prolonged storage. These changes were generally observed as both a decrease and a broadening of the melting range, suggesting partial hydrolysis back to the parent glycolic acid. From these observations, it was thereafter considered to be good practice to recrystallise the crude glycolide immediately after synthesis, store it under vacuum in a cool dark place, and then use it in subsequent polymerisation within a period of not longer than 1 week.

Based on these results, the conditions employed in RUN 3 were used to synthesize glycolide for the subsequent ring-opening polymerisation experiments which are now described.

3.3 Polymerisation of Glycolide

3.3.1 Introduction [3, 17-18, 23, 31-32, 43, 45-46, 48, 55-57]

3.3.1.1 Previous Work

As explained previously, high molecular weight poly(glycolic acid) is generally obtained from the ring-opening polymerisation of glycolide. According to the rather limited amount of literature information available in this field, the glycolide ring can open and polymerise in two possible ways : one is via acyl-oxygen bond cleavage (i.e., -CO-O-), while the other is via alkyl-oxygen bond cleavage (i.e., $-CH_2-O-$).

Based on the studies of model compounds, it was theorized that the mechanism based on alkyl-oxygen bond cleavage might be the more feasible energetically. However, it was later suggested by Cherdron and co-workers, as evidenced by their more definitive analytical studies, that acyl-oxygen bond cleavage was the preferred polymerisation mechanism [17, 44]. It has also been observed that the ring-opening polymerisation of glycolide bears some striking similarities to that of conventional six - membered ring lactones (e.g., δ-valerolactone). As shown by Bischoff and Walden, cyclic diesters, like monoesters, may undergo ring-opening polymerisation initiated by both anionic and cationic initiators [44].

It has been generally accepted for some time now that, in the case of cyclic diesters, high monomer conversions and polymer molecular weights will only be reached by conducting the reaction as a bulk polymerisation using chemical - complex initiators. Choosing the initiator for ring-opening polymerisation is important because of the influence it has on the end-groups, processability, molecular weight, molecular weight distribution, long-time stability, reactivity in different chemical/physical environments and even the total cost of the resulting polymer [45].

The earliest studies (1893) of Bischoff and Walden [3, 17, 23] described the transformation of glycolide into a polymer by either heating alone or in the presence of zinc chloride. High molecular weight polymers of glycolide have also been prepared by heating in the presence of metal oxides [44], while a more recent article described the polymerisation of glycolide with a triethylaluminium initiator [17]. In other studies, the polymerisation of glycolide to poly (glycolic acid) was performed in the presence of antimony trifluoride heated to 195 °C [33], at 220 °C using an organotin (II) compound [32, 43, 48, 55] such as stannous octoate, while combinations of stannous chloride dihydrate in alcohols have also been found to be very effective [31, 46, 56, 57].

3.3.1.2 Anionic Polymerisation

The nature of the actual initiation species, R^-, for most anionic polymerisation systems is still somewhat uncertain. Recent

studies by Furukawa et al [17] and Cherdron et al [17] have shown that the use of certain metal alkyls (such as aluminium alkyls) either alone or in combinations with water, oxygen and alcohol are active anionic - type initiators. According to Cherdron et al [17], the mechanism of initiation proposed for anionic polymerisation involves nucleophilic attack at the carbonyl carbon followed by acyl-oxygen cleavage of the ring, as shown below for δ-valeralactone. A similar mechanism may be assumed for glycolide polymerisation.

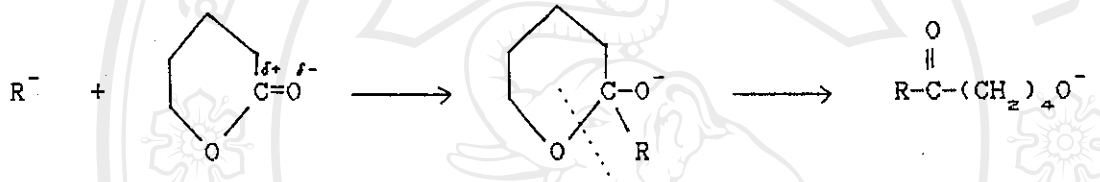

3.3.1.3 Cationic Polymerisation

In contrast, the cationic mechanism proposed by Cherdron et al [17] involves electrophilic attack of the carbonium ion of the initiator on the ring oxygen, again leading to cleavage of the acyl-oxygen bond. The acyl carbonium ion generated continues the reaction. For δ-valerolactone, and presumably for glycolide too, the initiation step may be represented as follows :

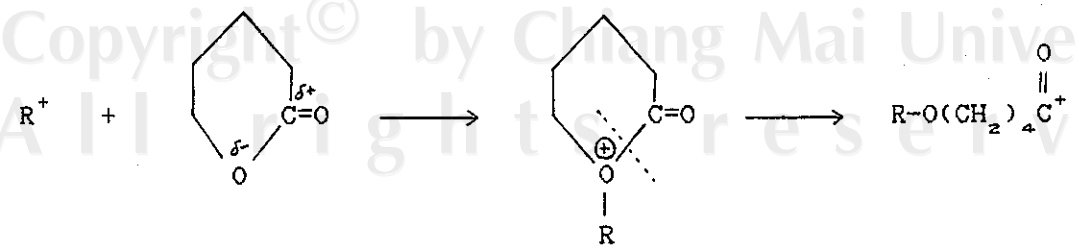

3.3.2 Experimental Aspects

3.3.2.1 Polymerisation using Aluminium Triethyl as Initiator

Approximately 2.0 g of pure glycolide were weighed into a 25 ml conical flask and a magnetic stirrer bar added. The flask was sealed with a 'Subaseal' and a stream of dry nitrogen gas continuously passed through the flask using syringe needles. The reaction flask and its contents were then immersed in a silicone oil bath at a temperature of 180 °C (± 5 °C) (see Fig. 3.4) until the glycolide had completely melted. Then, 0.01 ml of a 10% v/v aluminium triethyl initiator solution in dry decalin was rapidly injected into the stirred melt and the reaction mixture maintained at 180 °C for a period of up to 7 hours. The flask was then removed and allowed to cool to room temperature.

The polymer product obtained was purified by dissolving in hot dimethylsulfoxide (DMSO) as solvent at about 150 °C and then reprecipitating into an excess of stirred cooled methanol. After allowing to stand, filtering and washing with more methanol, the polymer was dried to constant weight in a vacuum oven at 80-90 °C. The final product was obtained as a finely-divided powder which varied in colour from cream to light tan as the polymerisation temperature increased.

Similar experiments at different polymerisation temperatures of 200 °C and 220 °C were also carried out according to this procedure.

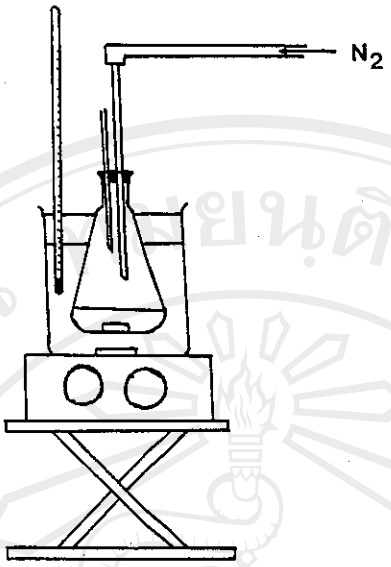

Fig. 3.4 : Apparatus used for the polymerisation of glycolide.

3.3.2.1.1 Polymer Characterisation

(A) Physical Characteristics

Table 3.3 describes the physical appearances of both the crude and purified PGA products. All products were solid powders which varied in colour according to the temperature and time of polymerisation. Generally speaking, the darker the colour, the more the polymer can be considered to have thermally degraded. Commercial PGA, as used in the manufacture of 'Dexon' sutures, is usually described as being "light tan" in colour.

Table 3.3 : Variation in colour of the poly(glycolic acid) products obtained at different polymerisation times and temperatures using aluminium triethyl as initiator.

Reaction Time (hrs)	180 °C		200 °C		220 °C	
	Crude PGA	Pure PGA	Crude PGA	Pure PGA	Crude PGA	Pure PGA
10 mins	cream	cream	cream	pale brown	pale brown	brown
30 mins	"	"	"	"	brown	"
1	pale yellow	"	"	"	"	"
2	"	"	"	"	"	"
3	"	"	pale brown	"	"	"
4	"	"	"	"	"	"
5	"	"	"	"	"	"
6	"	"	brown	"	"	"
7	"	"	"	"	dark brown	"

Note : all of the products were obtained in the form of solid powders after grinding and drying to constant weight in a vacuum oven at 90 °C.

(B) Structural Analysis by Infrared Spectroscopy

Figs. 3.5 and 3.6 show the infrared (IR) spectra of the poly(glycolic acid) products before and after purification respectively. The interpretation of these spectra is detailed in Table 3.4. The spectra were obtained with the samples in the form of KBr discs.

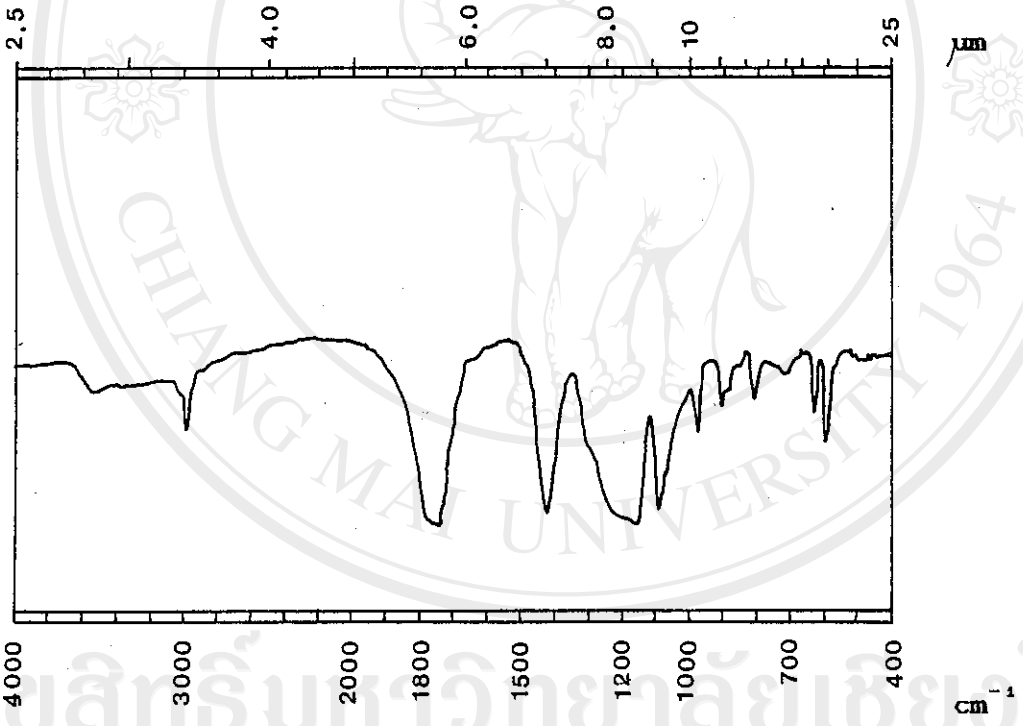

Fig. 3.5 : Infrared spectrum of crude PGA obtained using aluminium triethyl as initiator at 200 °C after 1 hour.

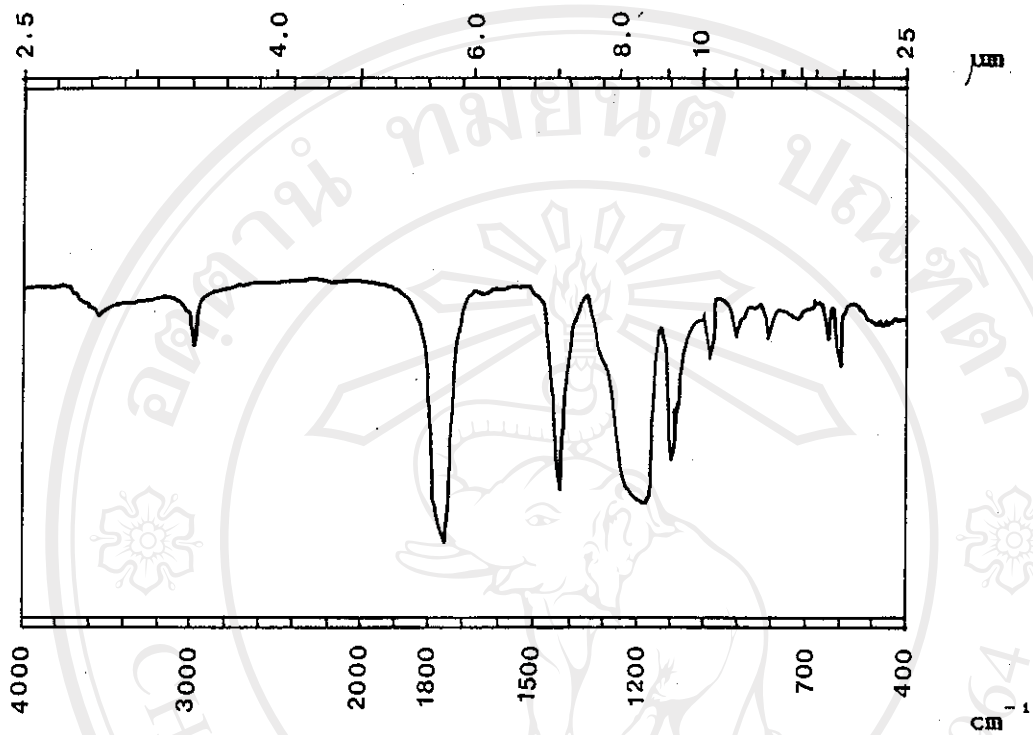

Fig. 3.6 : Infrared spectrum of purified PGA obtained using aluminium triethyl as initiator at 200 °C after 1 hour.

Table 3.4 : **Interpretation of infrared spectra of crude and purified poly(glycolic acid) products obtained using aluminium triethyl as initator.**

Vibrational Assignments	Wavenumber (cm^{-1})	
	Crude PGA	Purified PGA
O-H str. (end groups)	3700 - 3450	3700 - 3450
C-H str. in CH_2	2980	2980
C=O str.	1800 - 1720	1780 - 1740
C-H out-of-plane bend.	1420	1420
O-H in-plane bend.	1420 (coupled with C-H out-of-plane bending)	1420
C-O str.	1280 - 1140 [a] 1090 [b]	1260 - 1150 [a] 1100 [b]
O-H out-of-plane bend.	980 - 800	980 - 800

NOTES :

a = in acyl-oxygen bonds (i.e., $-\overset{O}{\overset{\|}{C}}-O-$)

b = in alkyl-oxygen bonds (i.e., $-\overset{H}{\overset{|}{\underset{H}{\underset{|}{C}}}}-O-$)

str. = stretching

bend. = bending

The IR spectra in Figs. 3.5 and 3.6 and the vibrational assignments in Table 3.4 are therefore seen to be consistent with the chemical structure of poly(glycolic acid).

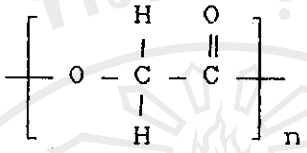

On comparing Figs. 3.5 and 3.6, the most obvious difference is that the band widths are narrower in the case of the purified polymer (Fig. 3.6). This is as would be expected since the main purpose of the purification procedure is to improve the chemical homogeneity of the polymer by removing any unreacted glycolide monomer and low molecular weight oligomeric species. Another significant feature worth noting is that the strong carbonyl C=O stretching band in the purified polymer spectrum (Fig. 3.6) is shifted to a slightly lower wavenumber (max. at 1750 cm^{-1}) than in the glycolide spectrum (Fig. 3.2/page 101; max. at 1770 cm^{-1}), presumably due to the release of ring strain on polymerisation.

(C) Melting Characteristics

The melting characteristics of the PGA products obtained via aluminium triethyl initiation were studied using two different techniques :

(1) Simple Visual Observation

In this method, the melting transition was observed visually using a Buchi SMP-20 Melting Point Determinator at a heating rate of 1 °C/min. Melting occurred over a range of temperature, as reported in Tables 3.5-3.7.

(2) Differential Scanning Calorimetry (DSC) [58-59]

In this more advanced technique, the melting ranges of the PGA products were determined from DSC curves recorded on a Perkin-Elmer DSC 7 Differential Scanning Calorimeter.

The following operating conditions were employed for each sample analysis :

Load Temp.	=	25 °C
Start Temp.	=	25 °C
Final Temp.	=	250 °C
Scanning Rate	=	10 °C/min
N_2 Purge Gas Pressure	=	20 psi
Coolant	=	ice-water
Sample Pan	=	aluminium
Sample Weight	=	5 mg (approx.)

The DSC melting points are reported in Tables 3.5-3.7 as the temperatures at the peak maxima (see Figs. 3.7-3.9). These were considered to be more meaningful for purposes of comparison than the

peak onset temperatures. The latter tended to vary inconsistently with changes in peak shape, partly as a result of the method by which the peak onset was calculated by the instrument's computer software. Selected examples of the DSC curves are shown in the form of overlays in Figs. 3.7-3.9.

(D) % Crystallinity

The percent crystallinities of the PGA products could be determined from the areas under the DSC melting peaks which are, in turn, directly proportional, in energy terms, to the heats of fusion.

From the "Polymer Handbook", 3rd edition [60], the heat of fusion of completely (i.e., 100%) crystalline PGA is given as 11 kJ/mol (i.e., per repeat unit molecular weight (58.04) in g). However, the units of the heat of fusion computed by the DSC instrument are given in units of " J/g " ; hence, from

$$11 \text{ kJ/mol} = 189.5 \text{ J/g}$$

$$\% \text{ crystallinity} = \frac{\text{heat of fusion of sample (J/g)}}{189.5 \text{ (J/g)}} \times 100 \%$$

The heats of fusion and percent crystallinities determined from the DSC curves are listed in Tables 3.5-3.7.

(E) Intrinsic Viscosity : Solomon-Ciuta One-Point Approximation Method [61-67]

Polymer intrinsic viscosities, which are directly related to the polymer molecular weights, were determined via dilute-solution viscometry using a Schott-Gerate AVS 300 Automatic Viscosity Measuring System.

Measurements were carried out on solutions prepared by dissolving the polymer at a temperature of 120 - 140 °C in dimethylsulfoxide (DMSO) as solvent at a single concentration of 0.5 g/dl. The flow-times of the polymer solution and of the DMSO solvent alone (t and t_o respectively) were then measured using a Schott-Gerate Ubbelohde Viscometer Type No. 531 03 (Capillary No. 0c) at a constant temperature of 90 ± 0.1 °C. The measured flow-times were corrected by using the Hagenbach Correction Table provided with the viscometer. High-temperature measurements were necessary in order to prevent the PGA from precipitating out of solution.

In this work, the intrinsic viscosity was calculated from the **SOLOMON CIUTA ONE-POINT EQUATION** [62] :

$$[\eta] = \frac{[\,2\,(\eta_{sp} - \ln \eta_{rel})\,]^{1/2}}{c} \qquad (3.1)$$

where ;

η_{rel} = relative viscosity = t / t_o

η_{sp} = specific viscosity = $\eta_{rel} - 1$

$[\eta]$ = intrinsic viscosity

c = concentration of polymer solution (g/dl)

The calculated values of $[\eta]$ are shown in Tables 3.5-3.7.

The Solomon-Ciuta One-Point Equation (3.1) has been widely used and, generally, gives good estimates of $[\eta]$ with good polymer-solvent systems which give thermodynamically stable solutions at the temperature of measurement. It is also found, in practice, that the estimates of $[\eta]$ are more accurate at a solution concentration for which $\eta_{sp} < 0.2$ [63]. Thus, η_{sp} must be measured with high precision, for which purpose automatic viscometers are best suited. The solution concentration of c = 0.5 g/dl chosen in this work is a typical concentration which is commonly used. However, it should also be noted that this method is usually considered to be accurate only when it is already known that there is a good linear relationship between c and η_{sp}/c and/or $(\ln \eta_{rel})/c$. This condition has been established in another research project carried out concurrently with this one [64].

Finally, the intrinsic viscosity, $[\eta]$, is related to the polymer molecular weight through the **MARK-HOUWINK-SAKURADA EQUATION** [65-67].

$$[\eta] = K\bar{M}_v^{a} \qquad (3.2)$$

where

$\bar{M}_v$ is the "viscosity-average molecular weight"

and K and a are interaction constants for a given polymer-solvent-temperature system. These constants are usually obtained from the "Polymer Handbook". Unfortunately, they are not available for PGA in any solvent and so, in this work, the actual polymer molecular weights cannot be calculated.

(**NOTE** : it might also be mentioned here that end-group analysis is also unsuitable since the exact nature of the chain end-groups from the ring-opening polymerisation of glycolide is unknown.)

Table 3.5 : Physical characterisation for poly(glycolic acid) initiated by aluminium triethyl at 180 °C.

Reaction Time (hrs)	MELTING POINT/RANGE, °C				CRYSTALLINITY				INTRINSIC VISCOSITY [η], dl/g
	from Buchi SMP-20		from DSC *		Crude PGA		Pure PGA		
	Crude	Pure	Crude	Pure	Heat of Fusion (J/g)	% Crystallinity	Heat of Fusion (J/g)	% Crystallinity	Pure PGA
10 mins	208-210	170-173							0.098
30 mins	208-211	172-175	219.95		88.61	46.8			0.133
1	209-212	160-163	218.56	203.83	60.97	32.2	101.04	53.3	0.040
2	210-214	160-163	219.95		89.44	47.2			
3	208-211	158-161							
4	208-212	160-163							0.040
5	208-211	159-162							
6	209-211	161-165							
7	209-211	161-165	220.39	205.27	101.08	53.3	95.26	50.3	0.040

* taken as temperature of melting peak maximum

Table 3.6 : Physical characterisation for poly(glycolic acid) initiated by aluminium triethyl at 200 °C.

Reaction Time	MELTING POINT/RANGE, °C				CRYSTALLINITY				INTRINSIC VISCOSITY
	from Buchi SMP-20		from DSC *		Crude PGA		Pure PGA		[η], dl/g
(hrs)	Crude	Pure	Crude	Pure	Heat of Fusion (J/g)	% Crystallinity	Heat of Fusion (J/g)	% Crystallinity	Pure PGA
10 mins	215-218	187-190							0.127
30 mins	214-216	182-185							0.052
1	214-217	180-183	218.58		94.69	50.0			0.028
2	211-214	180-184							
3	213-215	179-183							
4	215-217	180-183							0.028
5	214-216	180-183							
6	214-216	180-184							
7	215-217	181-184	223.77		101.54	53.6			0.028

* taken as temperature of melting peak maximum

Table 3.7 : Physical characterisation for poly(glycolic acid) initiated by aluminium triethyl at 220 °C.

Reaction Time (hrs)	MELTING POINT/RANGE, °C				CRYSTALLINITY				INTRINSIC VISCOSITY [η], dl/g
	from Buchi SMP-20		from DSC *		Crude PGA		Pure PGA		
	Crude	Pure	Crude	Pure	Heat of Fusion (J/g)	% Crystallinity	Heat of Fusion (J/g)	% Crystallinity	Pure PGA
10 mins	214-216	182-185							0.036
30 mins	215-218	187-190	211.55		92.84	49.0			0.044
1	207-210	186-190	210.75	199.45	93.24	49.2	81.24	42.9	0.042
2	205-208	185-188							
3	203-207	180-185							
4	204-207	177-181							0.044
5	206-210	177-181							
6	206-208	179-181							
7	209-213	186-190	216.55	207.72	76.80	40.5	92.30	48.7	0.052

* taken as temperature of melting peak maximum

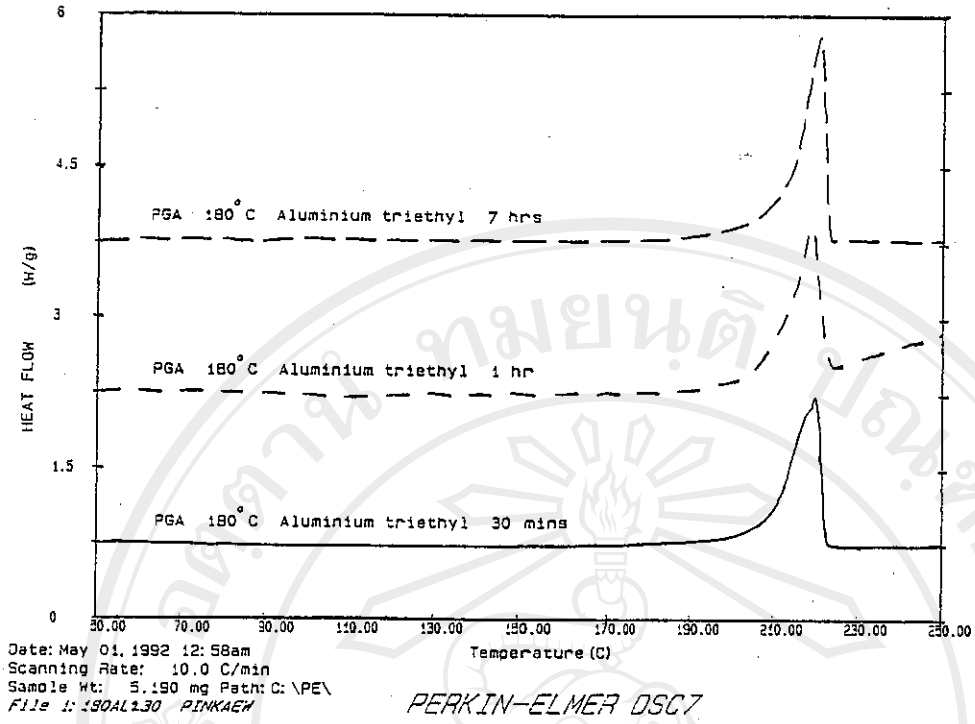

Fig. 3.7 : DSC curves of crude PGA initiated by aluminium triethyl showing the effect of reaction time.

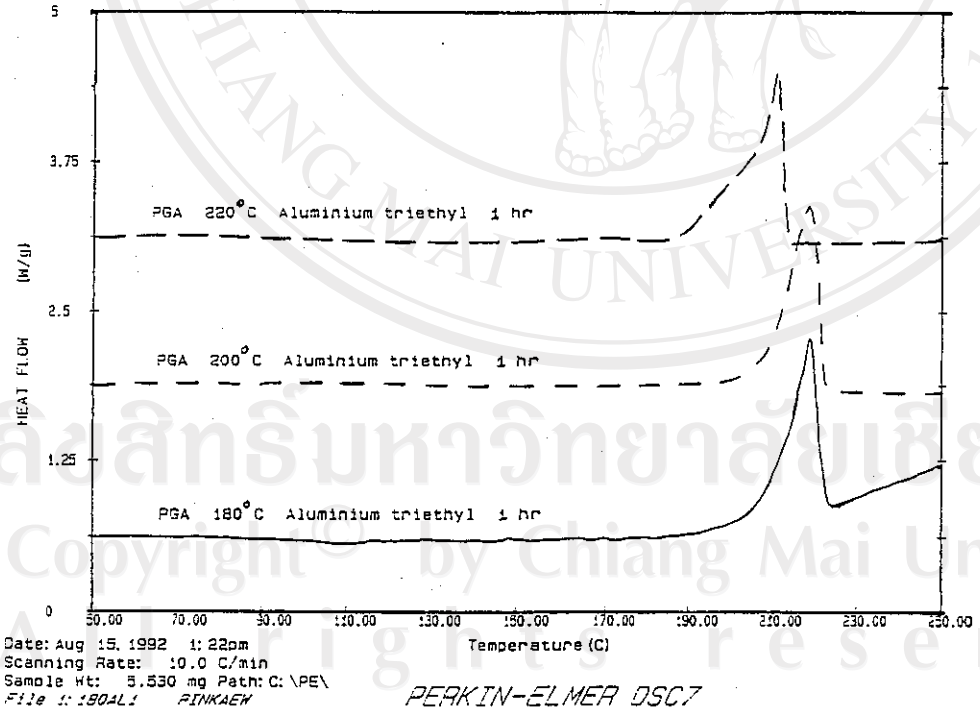

Fig. 3.8 : DSC curves of crude PGA initiated by aluminium triethyl showing the effect of reaction temperature.

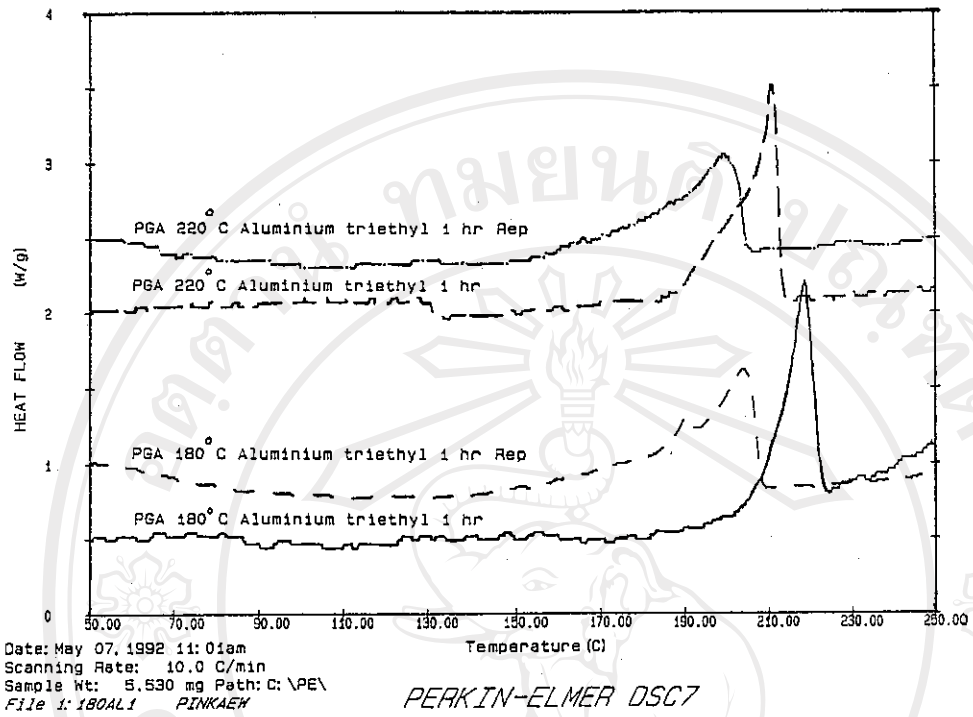

Fig. 3.9 : DSC curves of PGA initiated by aluminium triethyl showing the effect of purification by reprecipitation.

3.3.2.1.2 Discussion

The combined results of PGA physical characterisation presented in Tables 3.5-3.7 and Figs. 3.7-3.9 reveal some interesting features of the polymerisation reaction with respect to time and temperature. Additionally, the effects of purifying the crude PGA product by a conventional reprecipitation procedure are also described.

(1) Effect of Reaction Time

At a given temperature, the melting points/ranges of the polymer, whether observed visually (Buchi SMP-20) or determined analytically (DSC), show relatively little variation throughout the 7-hour course of the reaction. This indicates that, following polymerisation and subsequent solidification (usually within the first 5-10 minutes after injection of the initiator), the polymer's solid-state crystalline morphology is fully formed. As the DSC curves in Fig. 3.7 confirm, there is little change in the shape and position of the melting peak with increasing time, provided that thermal degradation of the polymer does not occur. This latter provision arises from the results in Table 3.7 which suggest that, at the highest reaction temperature of 220 °C, thermal degradation occurs at longer times, leading to a slight lowering of the observed melting range. This view is supported by the increasing brown discoloration of the PGA product at these longer times. Similarly, the small changes in intrinsic viscosity, $[\eta]$, suggest that, like the % crystallinity, the molecular weight of the polymer also increases very little once solidification has imposed severe restrictions on molecular motion in the solid state. There would therefore appear to be no particular advantage in continuing the reaction under these same conditions beyond a reaction time of about 2-3 hours.

(2) Effect of Reaction Temperature

It is noticeable in Tables 3.5 and 3.6 that, at 180 °C and 200 °C,

the polymer melting points/ranges, T_m, are significantly higher than the reaction temperatures, hence solidification occurred. However, at 220 °C, the results in Table 3.7 show a lowering in T_m below the reaction temperature, hence the system remained molten throughout. The obvious conclusion to be drawn from this is that there is an optimum reaction temperature at which a maximum T_m is obtained without accompanying thermal degradation. Of the three temperatures studied here, both 180 °C and 200 °C appear to give satisfactory results, while 220 °C is obviously too high. This effect is illustrated quite clearly by the DSC curves in Fig. 3.8. This highlights the importance of temperature selection and control in the case of polymers such as PGA which have narrow melt stability ranges.

(3) Effect of Purification

Normally, when polymers are purified by a reprecipitation procedure, their chemical homogeneity improves. This is commonly reflected in their improved physical appearance (e.g., lighter and more uniform in colour and particle size), higher average molecular weight (due to the removal of low molecular weight fractions), and higher and narrower melting ranges (less impurities, more uniform crystalline morphology). However, in this work, purification seems to have had some opposite effects. The most likely explanation for this seems to be that traces of the dimethylsulfoxide (DMSO) solvent used to dissolve the PGA still remained in contact with the polymer after purification. Indeed, the characteristically unpleasant odour of DMSO could still be detected in the reprecipitated PGA samples even after

prolonged vacuum drying at 90 °C for 20-30 hours. Trace solvent impurities would be expected to have the observed effects of both lowering and broadening the melting range in accordance with established laws of physical chemistry. These effects are clearly demonstrated in Fig. 3.9 for two different PGA samples, before and after reprecipitation.

From these results, it must be concluded that there are more disadvantages than advantages to the use of DMSO for PGA purification. Although DMSO is the most effective solvent known for PGA, it is very difficult to remove completely from the solid polymer, presumably due to strong polymer-solvent interactions. DMSO is a highly polar solvent due to the coordinate-covalent nature of its sulphur-oxygen bond and owes its solvating efficiency to the high electron density on the oxygen atom [68].

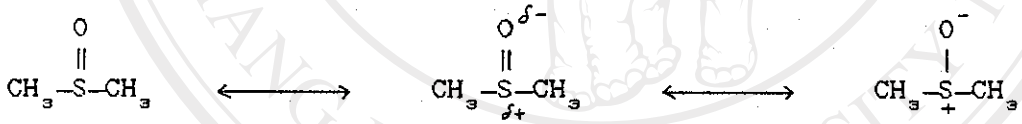

dimethylsulfoxide resonance forms

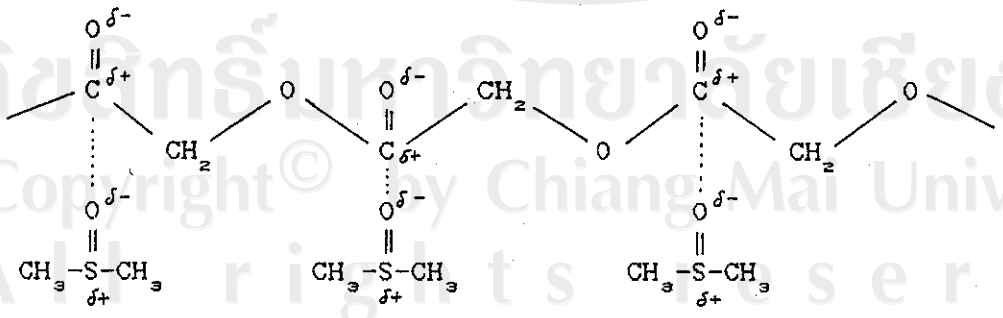

proposed solvation mechanism of PGA by DMSO (adapted from [68])

In this section, the ring-opening polymerisation of glycolide in bulk using aluminium triethyl, $Al(C_2H_5)_3$, as the initiator has been studied. It is well established that aluminium trialkyls containing linear alkyl groups are dimeric in solution [18, 23, 69] while those with branched alkyls are monomeric. Thus, $Al(C_2H_5)_3$ exists substantially in the dimeric form in hydrocarbon solvents [25] with the ethyl groups, formerly monovalent, acting as bridges with partial bonding to the aluminium atoms. The bond lengths are indicated in the structure below. As a general rule, the strength of the bond is inversely proportional to its length.

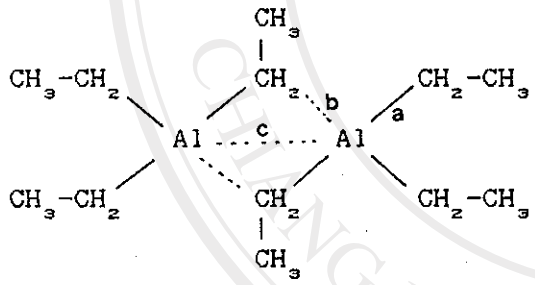

a = 200 pm

b = 224 pm

c = 255 pm

dimeric form of $Al(C_2H_5)_3$ in hydrocarbon solvents [25]

In this work, the $Al(C_2H_5)_3$ was prepared and handled as a 10% v/v solution in dry, distilled decalin under an inert atmosphere of dry nitrogen in a controlled atmosphere glove box. Pure $Al(C_2H_5)_3$ ignites spontaneously on contact with air and needs to be handled with extreme caution.

Generally, aluminium alkyls (AlR_3) are known as anionic initiators with the alkyl anion R^- as the initiating species. However, their anionic initiating efficiency is rather limited by the fact that, in solution, they exhibit a measurable dissociation only at very low concentrations. Consequently, it is generally accepted that the observed initiating efficiency of aluminium alkyls is due more to their combination with trace amounts of water present in the system as moisture impurities. Because they are strong Lewis acids, aluminium alkyls react strongly with water to form what is believed to be an alkyl aluminium oxide [17-18, 24, 44, 69].

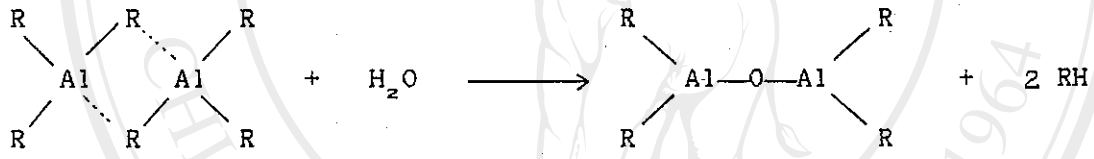

aluminium trialkyl (dimerized)

alkyl aluminium oxide

The nature of the initiating and propagating species differs considerably depending on the initiating system and reaction conditions. For this system, this alkyl aluminium oxide, $R_2AlOAlR_2$, becomes the active initiating species in the polymerisation reaction which is believed to proceed by a cationic mechanism through formation of an oxonium derivative of the monomer [18, 69]. In most cases, polymerisation appears to proceed by a coordination mechanism invoving

this initiating species [18].

The proposed mechanism for the aluminium triethyl initiated ring-opening polymerisation of glycolide is shown in Scheme 3.2, having been adapted from that reported for a similar system [23, 69]. There are apparently no kinetic termination reactions in this type of process, although chain transfer reactions are thought to occur, as indicated by a broad molecular weight distribution in the polymers formed. The main factors affecting molecular weight are the monomer-to-initiator ratio and the % conversion.

Initiation

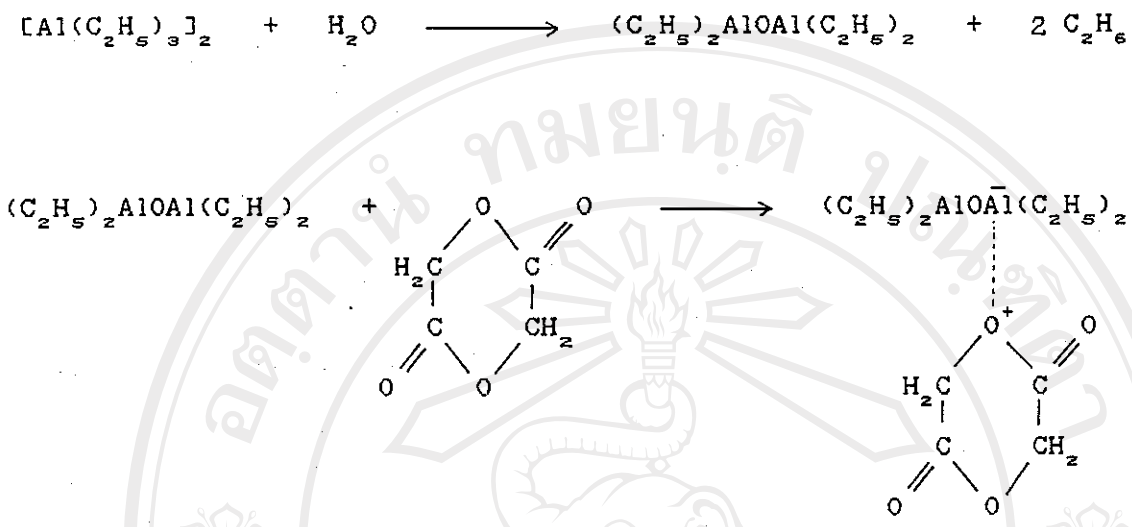

followed by

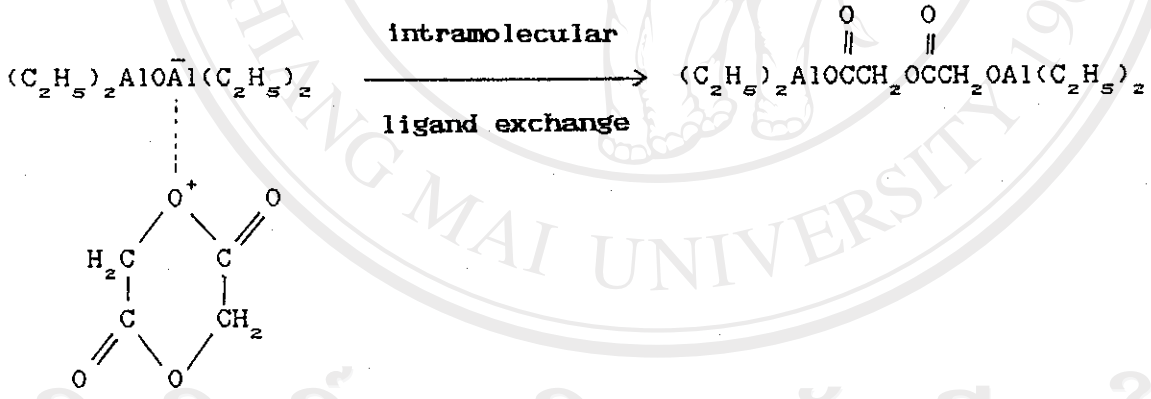

(...continued on next page)

Propagation

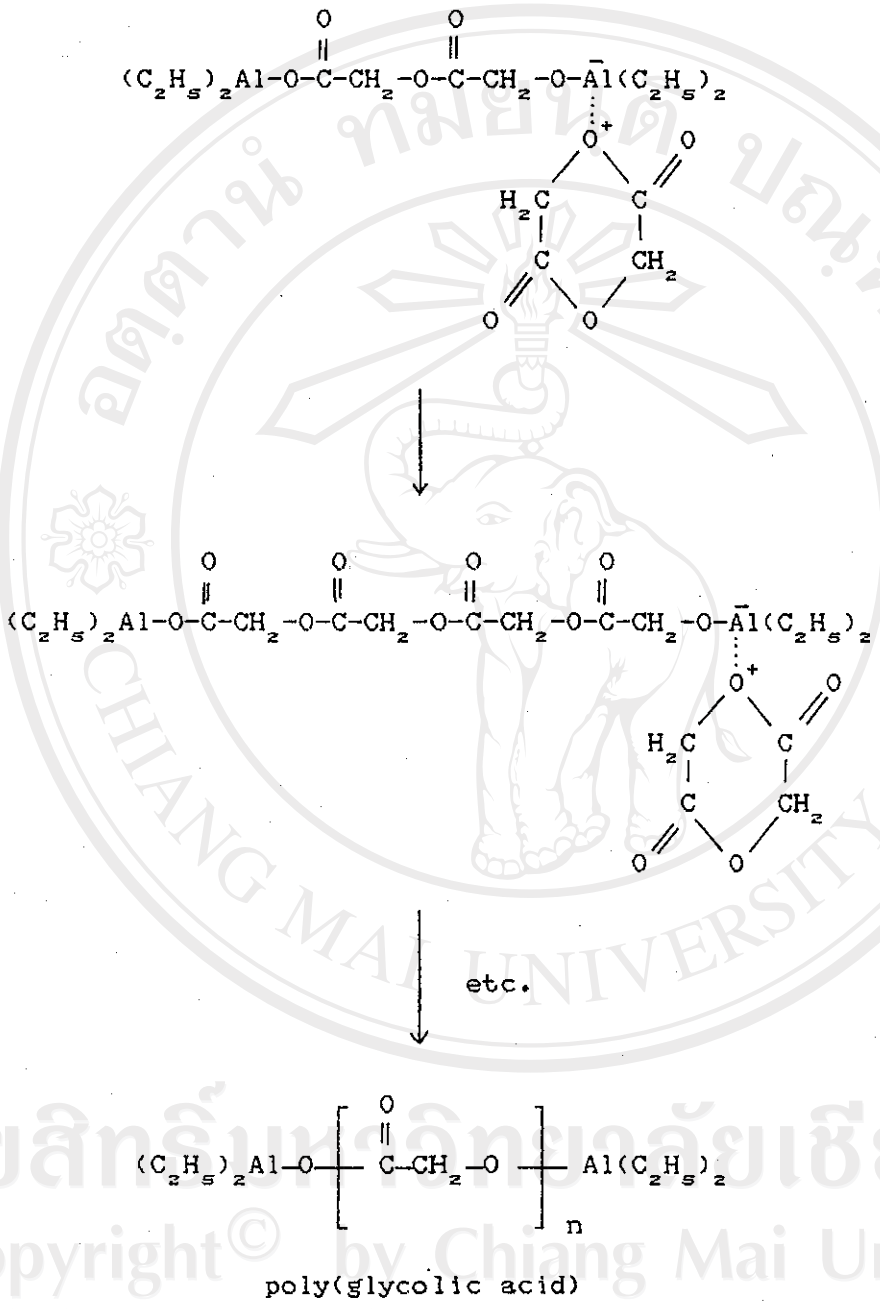

poly(glycolic acid)

Scheme 3.2 : Proposed mechanism for the aluminium triethyl initiated ring-opening polymerisation of glycolide.

In this mechanism, it must be emphasized that, in the formation of the active species, water does not act simply as a coinitiator in the normal sense of the term, i.e. it does not act simply as a proton donor in forming a complex to initiate the polymerisation. Instead, it actually reacts with the aluminium alkyl to form an entirely new species, an alkyl aluminium oxide, which serves as the initiator. For this reason, water has been termed a "modifier" for the aluminium alkyl instead of a "coinitiator". Furthermore, the ratio of the aluminium alkyl to the water appears to have an important influence on initiator activity. For example, a molar ratio of $[H_2O]$: $[Al(C_2H_5)_3]$ of 0.66 was reported to give both a maximum molecular weight and % conversion in the polymerisation of β-propiolactone at 50 °C [17]. However, a study of this dependence for glycolide was outside the scope of this project since it would have increased considerably the number of experiments which would have needed to be carried out. It should form the subject of a future study as an extension of this work.

Following these initiation steps, propagation occurs by glycolide monomer insertion at an aluminium-alkoxide bond [18]. This is then followed by an intramolecular rearrangement reaction to form a growing polymer chain having two aluminium alkyl end groups [23]. This type of monomer insertion mechanism has much in common with Ziegler-Natta polymerisation although it is not claimed to have the same stereoregulating effect.

3.3.2.2 Polymerisation using Antimony Trifluoride as Initiator

2.0 g of purified glycolide monomer were mixed with 0.030 g (1% by mole) of antimony trifluoride (SbF_3) initiator. The polymerisation procedure which followed and the conditions used were exactly the same as previously described in the preceding section 3.3.2.1.

3.3.2.2.1 Polymer Characterisation

(A) Physical characteristics

The physical appearances of the poly(glycolic acid) products which were obtained, both before and after purification, are described in Table 3.8. The gradual darkening in colour of the polymer with increasing reaction time and temperature was again taken as an indication of the increase in the extent of thermal degradation which had taken place.

Table 3.8 : Variation in colour of the poly(glycolic acid) products obtained at different polymerisation times and temperatures using antimony trifluoride as initiator.

Reaction Time (hrs)	180 °C		200 °C		220 °C	
	Crude PGA	Pure PGA	Crude PGA	Pure PGA	Crude PGA	Pure PGA
10 mins	pale cream	white	pale cream	white	pale cream	white
30 mins	"	"	"	"	"	"
1	"	"	"	"	"	"
2	"	"	"	"	cream	pale cream
3	"	"	cream	"	brown	brown
4	"	"	brown	brown	"	"
5	cream	"	"	"	dark brown	"
6	"	"	"	"	"	"
7	"	"	dark brown	"	"	"

Note : all of the products were obtained in the form of solid powders after grinding and drying to constant weight in a vacuum oven at 90 °C.

(B) Structural Analysis by Infrared Spectroscopy

Typical IR spectra of the PGA products from SbF_3 initiation are shown in Figs. 3.10 and 3.11. They are seem to be similar in every respect to those previously shown in Figs. 3.5 and 3.6 for the $Al(C_2H_5)_3$ - initiated products. Since the positions and shapes of the major bands are essentially the same, the spectra can be interpreted in identical fashion to that detailed in Table 3.4 previously and need not be repeated here.

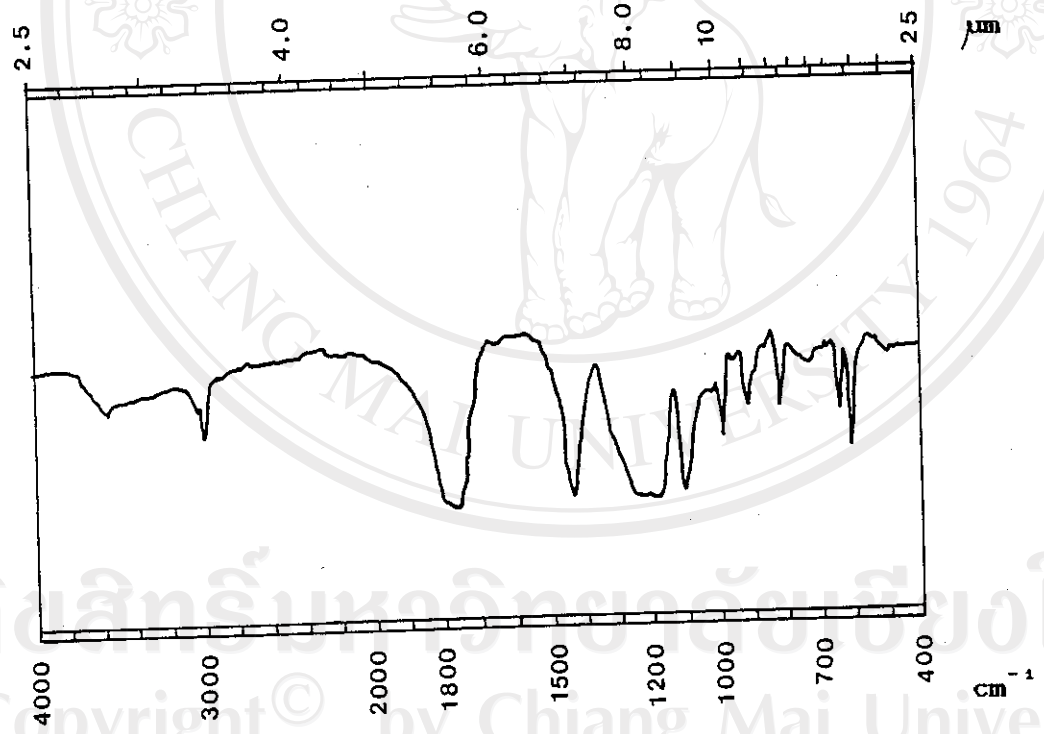

Fig. 3.10 : Infrared spectrum of crude PGA obtained using antimony trifluoride initiator at 200 °C after 1 hour.

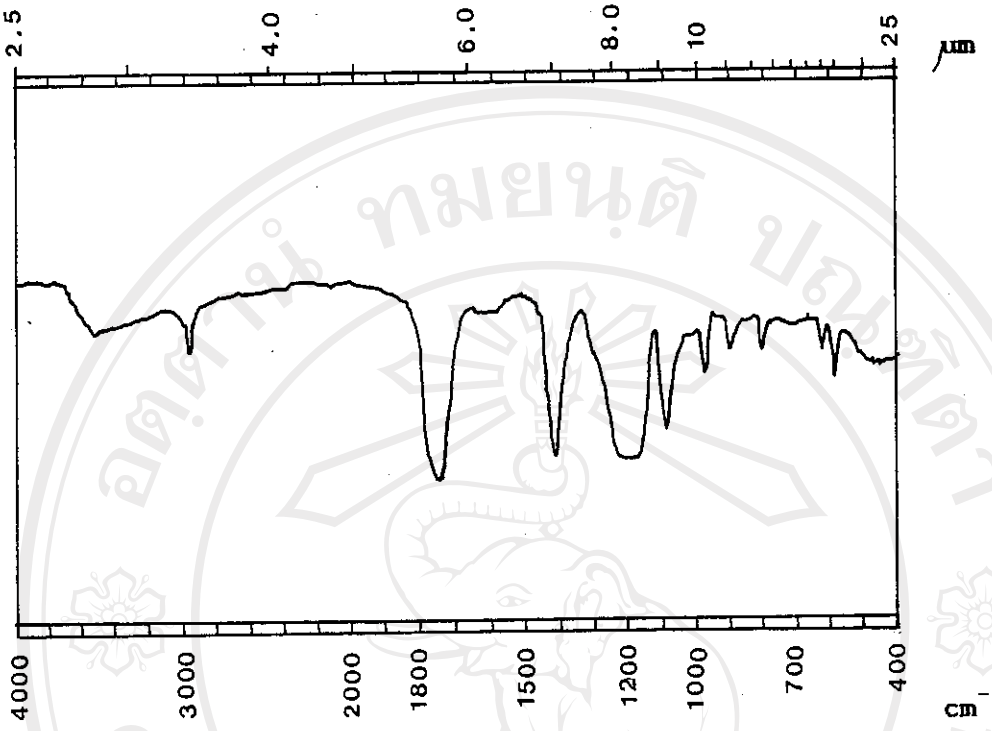

Fig. 3.11 : Infrared spectrum of purified PGA obtained using antimony trifluoride as initiator at 200 °C after 1 hour.

(C) Melting Characteristics

The melting characteristics of the PGA products obtained via SbF_3 initiation were studied in the same way as previously described for the $Al(C_2H_5)_3$ initiated products. The results obtained are given in Tables 3.9-3.11.

(D) **% Crystallinity**

The PGA heats of fusion and % crystallinities from DSC analysis are compared in Tables 3.9-3.11. The conditions of analysis were identical to those previously described and the results are therefore directly comparable with those in Tables 3.5-3.7.

(E) **Intrinsic Viscosity : Solomon-Cuita One-Point Approximation Method**

Single-concentration intrinsic viscosity measurements were carried out as previously described. The results obtained are given in Tables 3.9-3.11.

Table 3.9 : Physical characterisation for poly(glycolic acid) initiated by antimony trifluoride at 180 °C.

Reaction Time (hrs)	MELTING POINT/RANGE, °C				CRYSTALLINITY				INTRINSIC VISCOSITY [η], dl/g
	from Buchi SMP-20		from DSC *		Crude PGA		Pure PGA		
	Crude	Pure	Crude	Pure	Heat of Fusion (J/g)	% Crystallinity	Heat of Fusion (J/g)	% Crystallinity	Pure PGA
10 mins	210-214	171-175							0.032
30 mins	213-216	178-182							0.036
1	207-210	179-181	215.25		108.44	57.2			0.071
2	206-210	182-185							
3	208-211	180-183							0.135
4	210-214	181-184							0.164
5	208-211	180-184							
6	208-212	181-183							
7	209-212	182-185	216.18	202.48	115.54	61.0	97.71	51.6	0.188

* taken as temperature of melting peak maximum

Table 3.10 : Physical characterisation for poly(glycolic acid) initiated by antimony trifluoride at 200 °C.

Reaction Time	MELTING POINT/RANGE, °C				CRYSTALLINITY				INTRINSIC VISCOSITY [η], dl/g
	from Buchi SMP-20		from DSC *		Crude PGA		Pure PGA		
(hrs)	Crude	Pure	Crude	Pure	Heat of Fusion (J/g)	% Crystallinity	Heat of Fusion (J/g)	% Crystallinity	Pure PGA
10 mins	212-215	175-179							0.040
30 mins	214-217	178-182	221.11		100.15	52.8			0.046
1	213-216	182-185	221.28	193.94	85.89	45.3	110.46	58.3	0.075
2	204-209	174-178							
3	209-215	175-178							0.082
4	211-217	177-180							0.118
5	214-217	178-181							
6	214-218	179-183							
7	215-218	181-184	226.16		109.88	58.0			0.171

* taken as temperature of melting peak maximum

Table 3.11 : Physical characterisation for poly(glycolic acid) initiated by antimony trifluoride at 220 °C.

Reaction Time (hrs)	MELTING POINT/RANGE, °C				CRYSTALLINITY				INTRINSIC VISCOSITY [η], dl/g
	from Buchi SMP-20		from DSC *		Crude PGA		Pure PGA		
	Crude	Pure	Crude	Pure	Heat of Fusion (J/g)	% Crystallinity	Heat of Fusion (J/g)	% Crystallinity	Pure PGA
10 mins	206-210	151-154	222.39		88.47	46.7			0.018
30 mins	208-211	138-141							0.016
1	204-209	139-142							0.098
2	204-208	139-142							
3	204-208	138-144							0.118
4	205-209	139-143							0.167
5	205-208	140-143							
6	206-208	145-148							
7	206-209	145-150	218.51	194.41	88.44	46.7	98.26	51.8	0.201

* taken as temperature of melting peak maximum

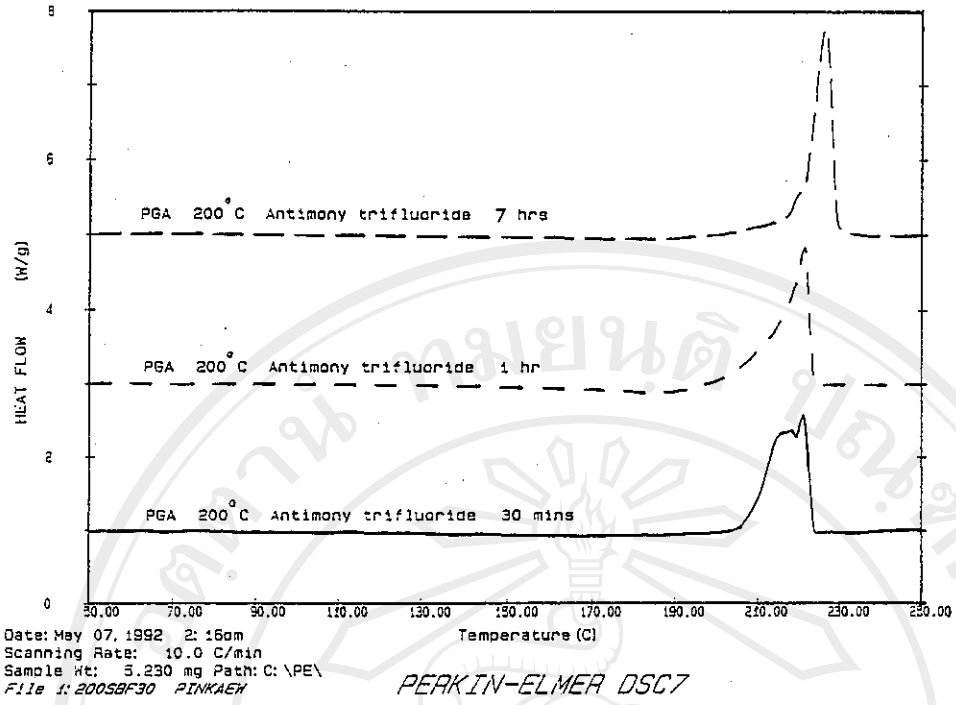

Fig. 3.12 : DSC curves of crude PGA initiated by antimony trifluoride showing the effect of reaction time.

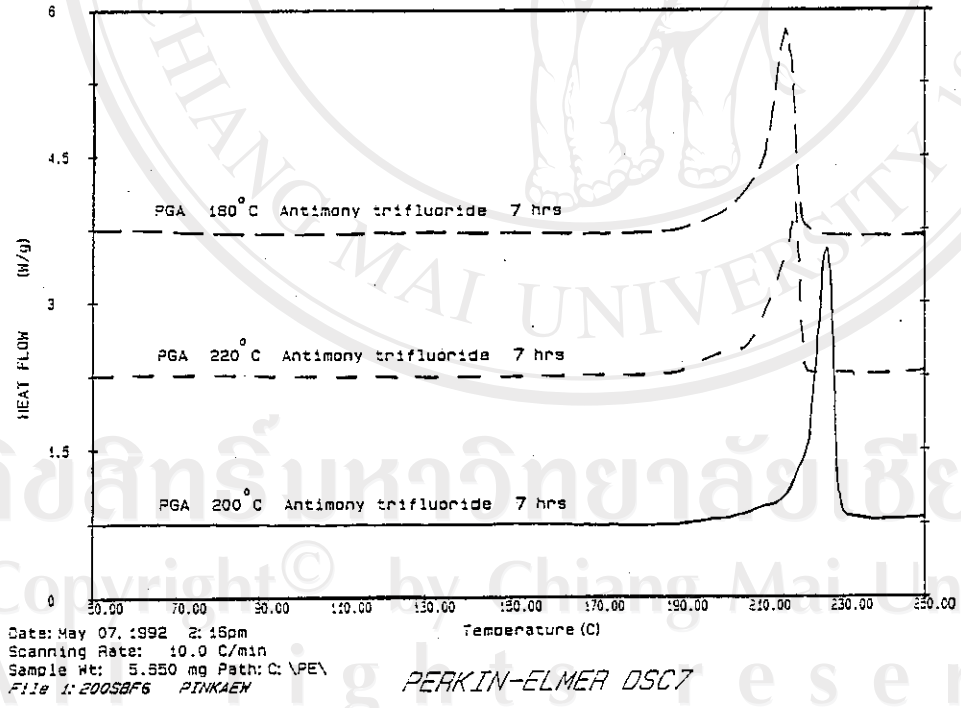

Fig. 3.13 : DSC curves of crude PGA initiated by antimony trifluoride showing the effect of reaction temperature.

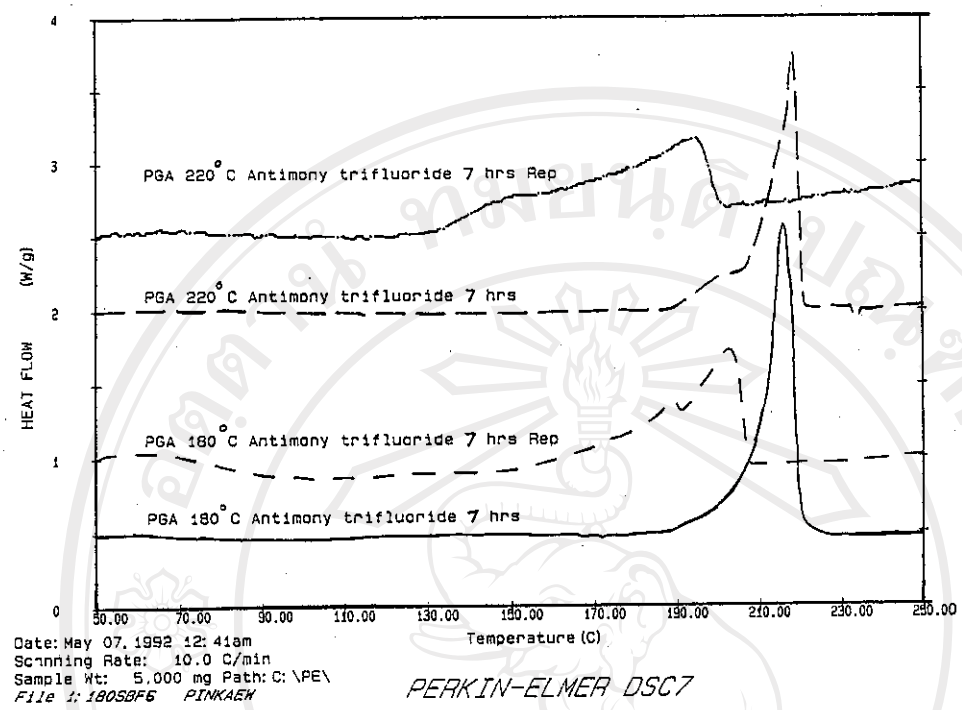

Fig. 3.14 : DSC curves of PGA initiated by antimony trifluoride showing the effect of purification by reprecipitation.

3.3.2.2.2 Discussion

The combined results of PGA physical characterisation presented in Tables 3.9 - 3.11 and Figs. 3.12 - 3.14 illustrate the effects of reaction time and temperature. In addition, the effect of purifying the crude PGA product by a conventional reprecipitation procedure is also shown.

(1) Effect of Reaction Time

At a given temperature, the melting points/ranges of the polymer products, whether observed visually (Buchi SMP-20) or determined analytically (DSC), show relatively little variation throughout the 7-hour course of the reaction. This again indicates that, following polymerisation and subsequent solidification (usually within the first 10-15 minutes at 180 °C and within about 1 hour at 200 °C after addition of the initiator), the establishment of the polymer's solid-state crystalline morphology is well advanced. This is supported by the top two DSC curves in Fig. 3.12 which confirm that there is relatively little change in the shape and position of the melting peak with increasing time (1 ⟶ 7 hours) after solidification, provided that thermal degradation of the polymer does not occur. The slight changes that do occur can be attributed to a gradual narrowing of the size distribution of the crystalline regions in the solid state by the process of annealing. In contrast, at the highest temperature of 220 °C, the initial melting point after the first 10 minutes later decreased, indicating that thermal degradation occurred at longer times. This view is supported by the increasing dark brown discoloration of the PGA product.

(2) Effect of Reaction Temperature

It is shown in Tables 3.9-3.10 that, at 180 °C and 200 °C, the polymer melting points/ranges, T_m, tend to increase with increasing temperature of polymerisation provided that thermal degradation does

not intervene. Solidification occurs when the polymer molecular weight reaches a level at which the polymer's T_m exceeds the reaction temperature. Thus, the choice of reaction temperature has an important effect on the properties of the final product.

According to the DSC curves in Fig. 3.13, a temperature of 200 °C appears to give the best results in terms of the highest T_m without thermal degradation. Thermal degradation sets in at 220 °C.

(3) **Effect of Purification**

Purification of the polymer by reprecipitation from DMSO again lowered and broadened its melting range relative to the crude product, as previously described for $Al(C_2H_5)_3$ as initiator. These effects are again clearly shown in Fig. 3.14 for two different PGA samples, before and after reprecipitation.

(4) **Effect of Initiator**

Comparing the $Al(C_2H_5)_3$ and SbF_3 initiators, $Al(C_2H_5)_3$ gave the higher melting point polymer (from DSC) at 180 °C, while at 200 °C, SbF_3 gave the higher T_m. From these results, using SbF_3 as initiator at 200 °C seems to be better from the point of view of the polymer's melting characteristics; however, the physical appearance of the final product (crude) showed more discoloration than when using $Al(C_2H_5)_3$. Both initiators are therefore considered to be effective in glycolide polymerisation, with the action of $Al(C_2H_5)_3$ being the more widely documented in the literature.

In the case of using antimony trifluoride (SbF_3) as initiator, the mechanism of initiation is believed to be cationic in nature. Antimony trifluoride, being a strong Lewis acid (electron acceptor), readily combines with a second component termed a "cocatalyst" or "coinitiator" which is a proton donor (protogen). Even trace amounts of water (or alcohol, organic acids) present in the system can form an ion pair of a proton-cation complex which becomes the actual initiating species. This ion pair is capable of initiating the cationic ring-opening polymerisation; however, an excess of the coinitiator can destroy the catalytic properties of the system. In the SbF_3-initiated ring-opening polymerisation of glycolide, the proposed mechanism of the reaction is as shown in Scheme 3.3 [18, 20, 23-24, 44].

Initiation

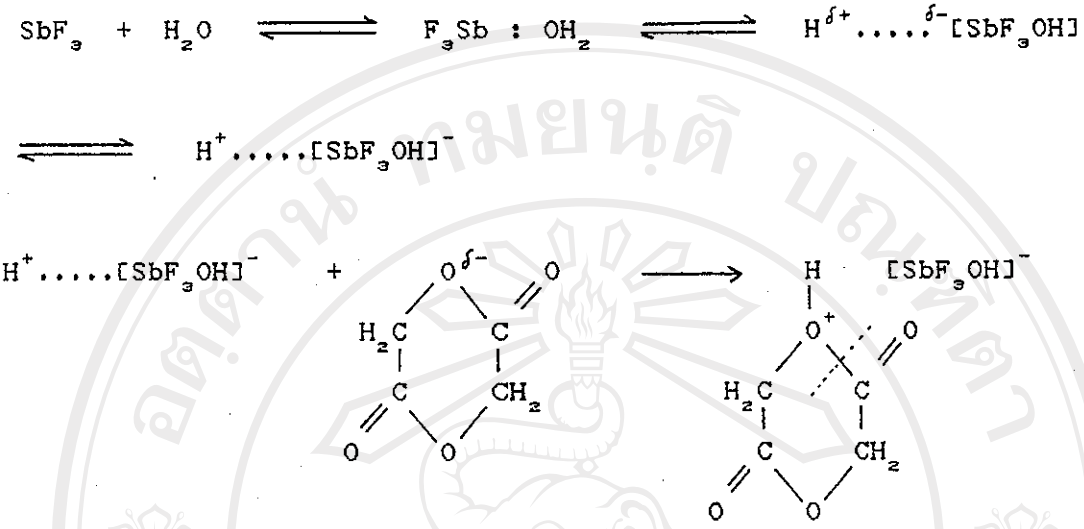

followed by

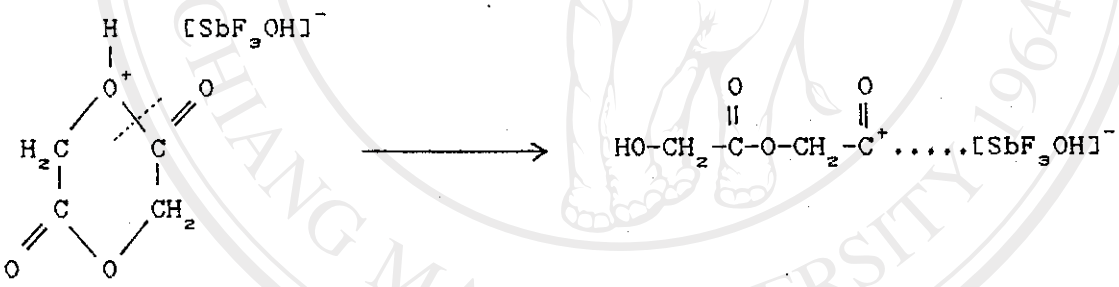

Propagation

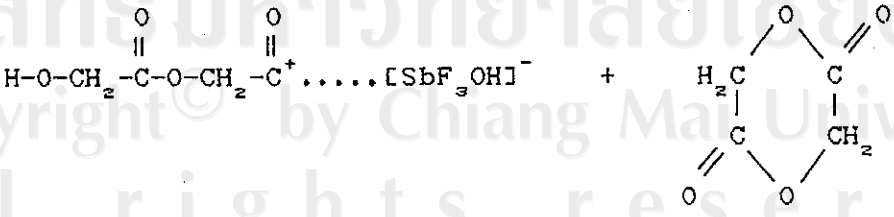

(...continued on next page)

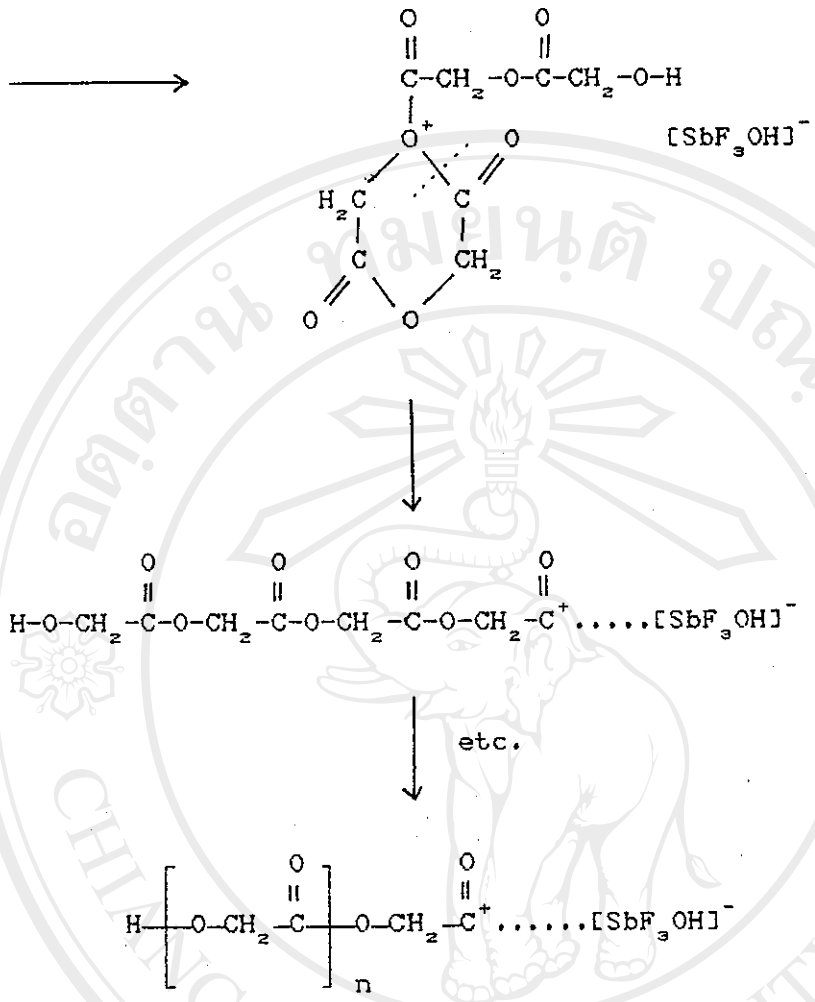

etc.

Termination (e.g., with counterion)

Scheme 3.3 : Proposed mechanism for the antimony trifluoride initiated cationic ring-opening polymerisation of glycolide.

In this proposed mechanism, initiation actually involves two sequential steps : (1) the generation of a proton which is the active species and (2) the addition of that proton to the monomer. Lewis acids, such as SbF_5, interact first with the coinitiator (water) to produce a proton donator (active species) by a reaction called a "coinitiation process" [18].

$$SbF_5 + H_2O \longrightarrow F_5Sb : OH_2 \rightleftharpoons [F_5SbOH]^- + H^+$$

The Lewis acid may conceivably act as both the initiator and coinitiator in the coinitiation process if it can self-ionize. It may then be able to initiate polymerisation by the direct addition of initiator to monomer. However, much of the experimental evidence to support this self-ionization process is indirect for reaction systems at different levels of dryness and purity. The weight of evidence suggests, therefore, that if self-ionization does occur, its contribution to the overall initiation process is small when a proton or cation donor is present.

SbF_5 does not normally function as an initiator in the absence of a coinitiator such as water. However, even when such a coinitiator is not deliberately added to the system, enough adsorbed water molecules are present on the inside surface of the apparatus to coinitiate the reaction. The polymerisation rate increases with increasing [initiator] / [coinitiator], but it can be shown that an optimum ratio of initiator to coinitiator exists (often 1:1) that gives a maximum reaction rate and then either decreases or levels off.

Large amounts of coinitiator decrease the reaction rate by destruction of the initiator. Lowering of the coinitiator concentration below the optimum amount lowers the polymerisation rate, as shown in Figure below [20].

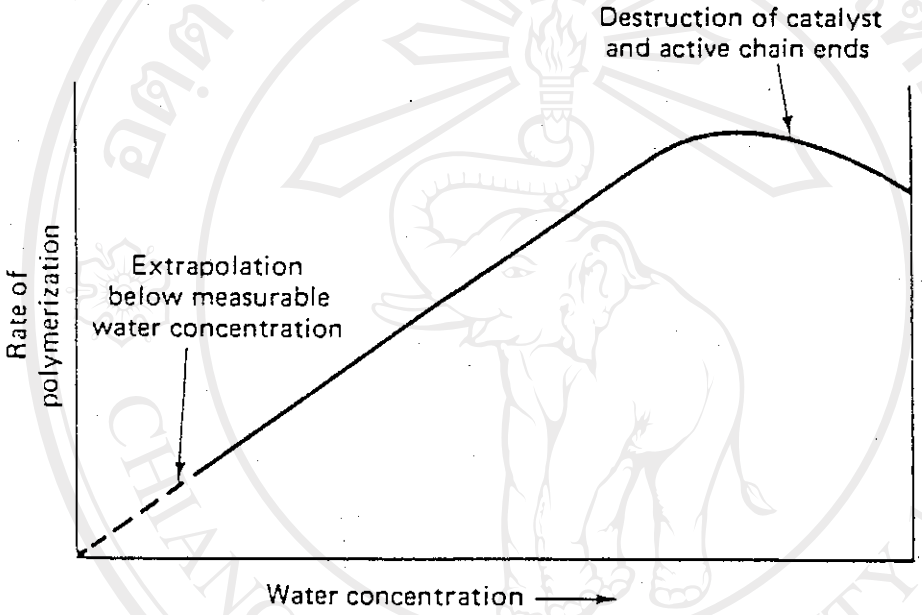

Showing the falloff in the rate of a cationic polymerisation as the amount of the cocatalysts (water) is reduced below the optimum ratio. See, for example, papers by A. G. Evans and G. W. Meadows. Trans. Faraday Soc., 46, 327 (1950), and A. M. Eastham, J. Am. Chem. Soc., 78, 6040 (1956).

The very lowest coinitiator concentration cannot be attained reproducibly, but extrapolation of the curve strongly suggests that the polymerisation rate would be zero in the complete absence of a coinitiator. The optimum initiator to coinitiator ratio varies considerably depending on the initiator, coinitiator, monomer, solvent (if used) and temperature, since these factors affect the balance between the competing processes of initiation and inactivation. Thus, for practical purposes, nearly all cationic initiators can be considered as species of the general formula H^+X^-. However, in this work, the exact amount of water present in the system was not known and so the initiator to coinitiator ratio cannot be quantified. This may form the subject of a future research project.

From the coinitiation process, the H^+ proton is thought to be the actual initiating species, abstracting a pair of electrons from the monomer and giving a cationic chain end which reacts with additional monomer molecules by electrophilic attack [70]. In the case of glycolide, this would probably lead to ring-opening via acyl-oxygen bond scission [44].

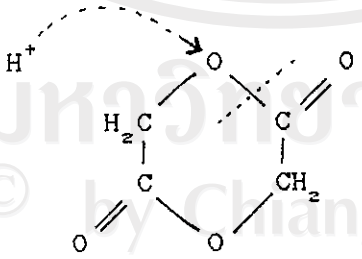

Propagation then takes place by successive insertion of glycolide monomer molecules into the cation-anion bond between the

growing cationic chain-end and its negative counterion. Electrophilic attack by the terminal cation on the next glycolide monomer then occurs, and so on.

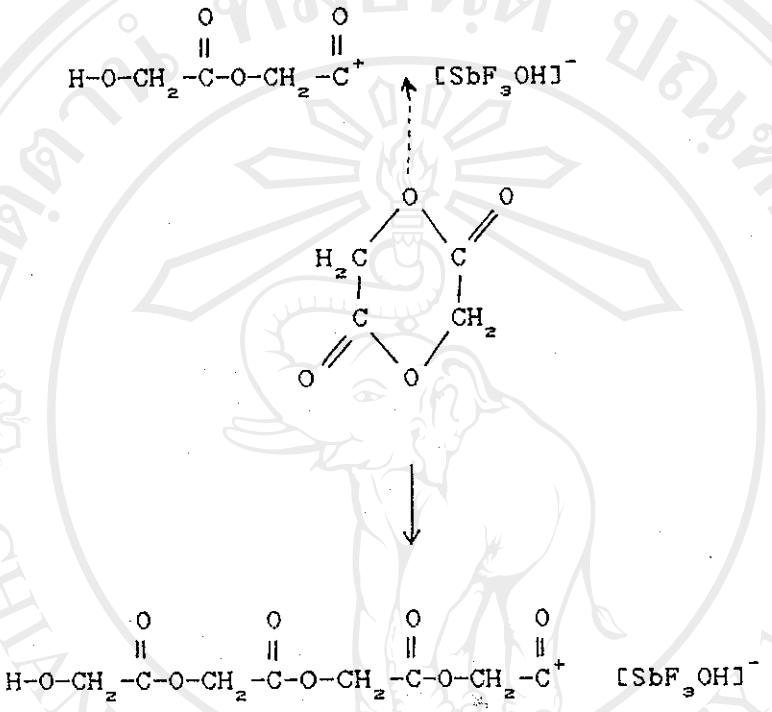

Termination of the chain growth process in cationic polymerisation occurs mainly as a result of chain transfer or by some effect due to the negative counterion. The latter reaction includes the loss of a proton to the negatively-charged counterion which is electrostatically held near the growing chain and so can exert a steric influence on the addition of monomer units [70]. Another possibility is that the counterion may actually terminate the reaction species by anion transfer, e.g.,

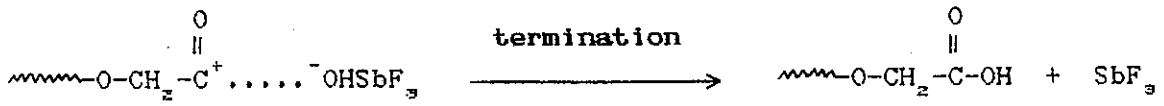

Either of these two counterion effects would lead to inhibition of the propagation step resulting in low molecular weight polymer formation.

Termination can also take place by the reaction of a growing chain end with traces of water or other protonic reagents which have varying chain transfer properties. For example, termination by water impurities involves transfer of an OH group to the propagating cation chain.

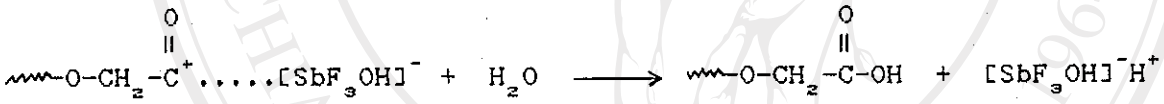

This proposed mechanism for the SbF_5-initiated ring-opening polymerisation of glycolide is mainly adapted from those proposed in the literature for similar systems. The specific properties of SbF_5 and glycolide have been taken into consideration for each of the reaction steps. However, confirmation of this mechanism will require more detailed studies to be carried out in a future research project.

3.3.2.3 Polymerisation using Stannous Octoate as Initiator

To 2.0 g of pure glycolide were added 0.070 g (1% by mole) of stannous octoate as initiator. Apart form this, the experimental procedure and conditions of polymerisation were the same as previously described in 3.3.2.1 for aluminium triethyl initiation.

3.3.2.3.1 Polymer Characterisation

(A) Physical Characteristics

The physical appearances of the PGA products are compared in Table 3.12. The gradual darkening in colour of the polymer product with increasing reaction time and temperature was considered to be due to an increase in the extent of thermal degradation.

Table 3.12 : Variation in colour of the poly(glycolic acid) products obtained at different polymerisation times and temperature using stannous octoate as initiator.

Reaction Time (hrs)	180 °C		200 °C		220 °C	
	Crude PGA	Pure PGA	Crude PGA	Pure PGA	Crude PGA	Pure PGA
10 mins	pale cream	white	pale brown	cream	dark brown	cream
30 mins	"	"	"	"	brown-black	brown
1	"	"	"	pale brown	"	"
2	cream	"	brown	"	"	"
3	"	"	"	"	"	"
4	"	"	"	"	"	"
5	"	"	dark brown	"	"	"
6	"	"	brown-black	"	"	"
7	"	"	"	"	"	"

Note : all of the products were obtained in the form of solid powders after grinding and drying to constant weight in a vacuum oven at 90 °C.

(B) Structural Analysis by Infrared Spectroscopy

The IR spectra obtained were very similar with respect to the positions of the major bands to the spectra previously shown for the aluminium triethyl and antimony trifluoride initiated polymerisations. An example is shown in Fig. 3.15.

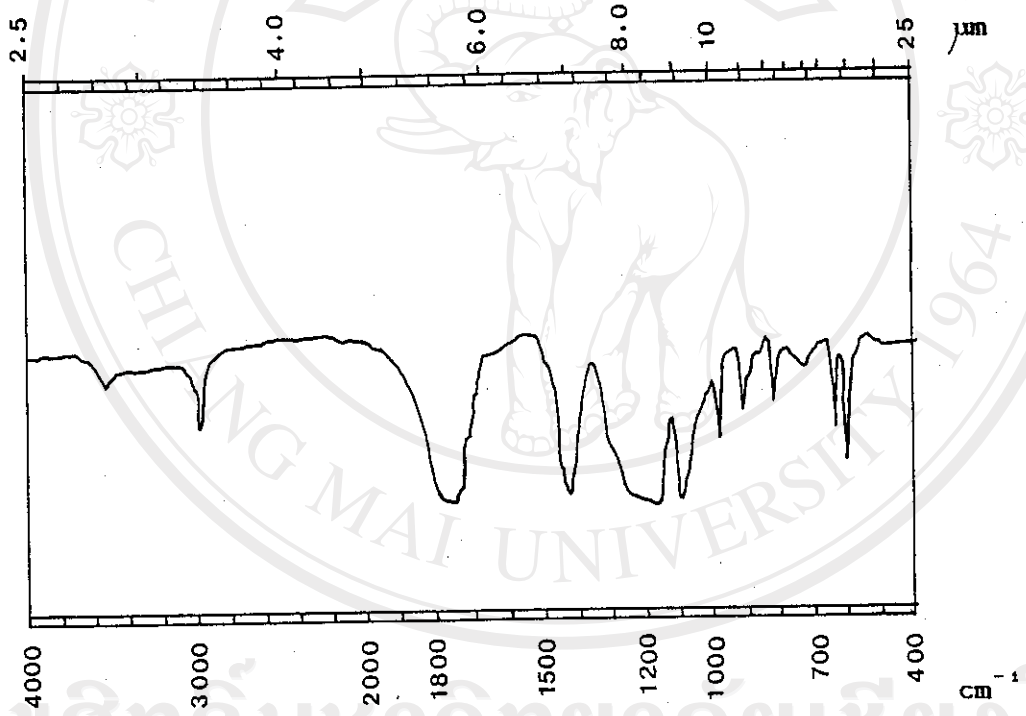

Fig. 3.15 : Infrared spectrum of crude PGA obtained using stannous octoate as initiator at 200 °C after 1 hour.

(C) Melting Characteristics

The melting characteristics of the PGA products obtained via stannous octoate initiation were studied as previously described. The results are given in Tables 3.13-3.15.

(D) % Crystallinity

The heats of fusion and corresponding % cyrstallinities from DSC are compared in Tables 3.13-3.15 and curve overlays shown in Figs. 3.16-3.18.

(E) Intrinsic Viscosity : Solomon-Ciuta One-Point Approximation Method

The results of the single-concentration intrinsic viscosity determinations are also shown in Tables 3.13-3.15.

Table 3.13 : Physical characterisation for poly(glycolic acid) initiated by stannous octoate at 180 °C.

Reaction Time (hrs)	MELTING POINT/RANGE, °C				CRYSTALLINITY				INTRINSIC VISCOSITY [η], dl/g
	from Buchi SMP-20		from DSC *		Crude PGA		Pure PGA		
	Crude	Pure	Crude	Pure	Heat of Fusion (J/g)	% Crystallinity	Heat of Fusion (J/g)	% Crystallinity	Pure PGA
10 mins	209-215	185-188							0.123
30 mins	210-216	165-168	223.59		102.05	53.8			0.026
1	213-216	166-169							0.032
2	216-218	165-168							
3	215-217	161-164							
4	208-213	160-163							0.032
5	209-213	160-163							
6	208-212	160-163							
7	209-212	161-164	213.50	217.01	117.01	61.8	119.42	63.0	0.032

* taken as temperature of melting peak maximum

Table 3.14 : Physical characterisation for poly(glycolic acid) initiated by stannous octoate at 200 °C.

Reaction Time (hrs)	MELTING POINT/RANGE, °C				CRYSTALLINITY				INTRINSIC VISCOSITY [η], dl/g
	from Buchi SMP-20		from DSC *		Crude PGA		Pure PGA		
	Crude	Pure	Crude	Pure	Heat of Fusion (J/g)	% Crystallinity	Heat of Fusion (J/g)	% Crystallinity	Pure PGA
10 mins	213-216	187-191							0.064
30 mins	215-217	189-193							0.071
1	212-215	184-187	214.99	211.50	90.35	47.7	104.34	55.1	0.046
2	210-215	180-184							
3	210-214	180-183							
4	212-215	184-187							0.048
5	213-216	185-188							
6	213-215	186-190							
7	213-216	186-189	222.77		107.72	56.8			0.050

* taken as temperature of melting peak maximum

Table 3.15 : Physical characterisation for poly(glycolic acid) initiated by stannous octoate at 220 °C.

Reaction Time (hrs)	MELTING POINT/RANGE, °C				CRYSTALLINITY				INTRINSIC VISCOSITY [η], dl/g
	from Buchi SMP-20		from DSC *		Crude PGA		Pure PGA		
	Crude	Pure	Crude	Pure	Heat of Fusion (J/g)	% Crystallinity	Heat of Fusion (J/g)	% Crystallinity	Pure PGA
10 mins	214-216	161-164							0.063
30 mins	206-212	159-162	219.10		84.83	44.8			0.014
1	207-210	160-163							0.036
2	202-206	157-160							
3	202-204	154-158							
4	203-206	155-160							0.038
5	205-210	160-165							
6	210-212	175-180							
7	212-214	178-182	224.81	213.36	94.29	49.8	119.75	63.2	0.040

* taken as temperature of melting peak maximum

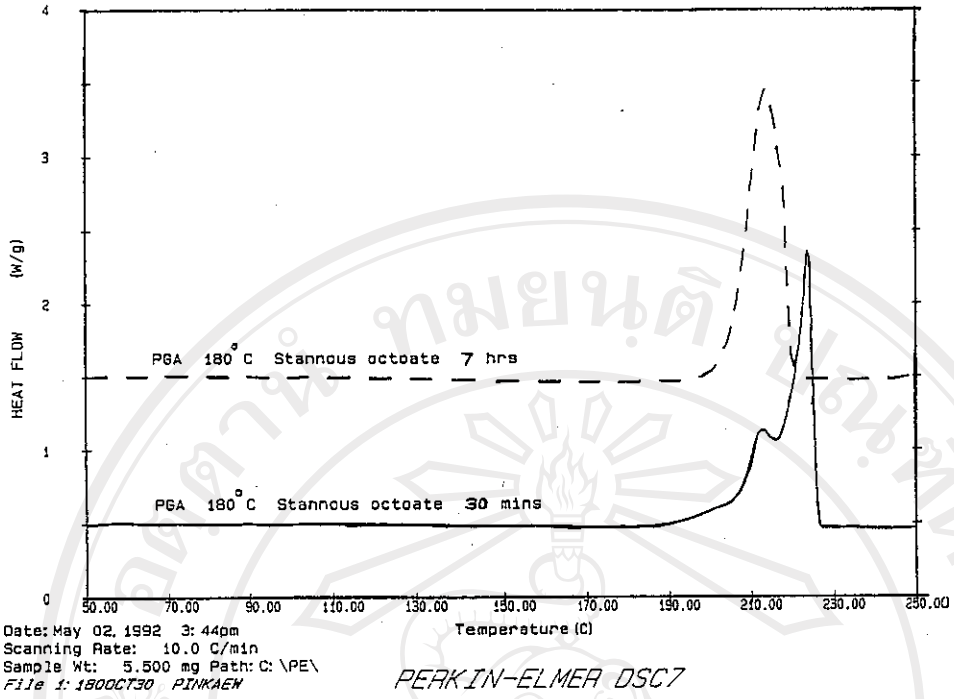

Fig. 3.16 : DSC curves of crude PGA initiated by stannous octoate showing the effect of reaction time.

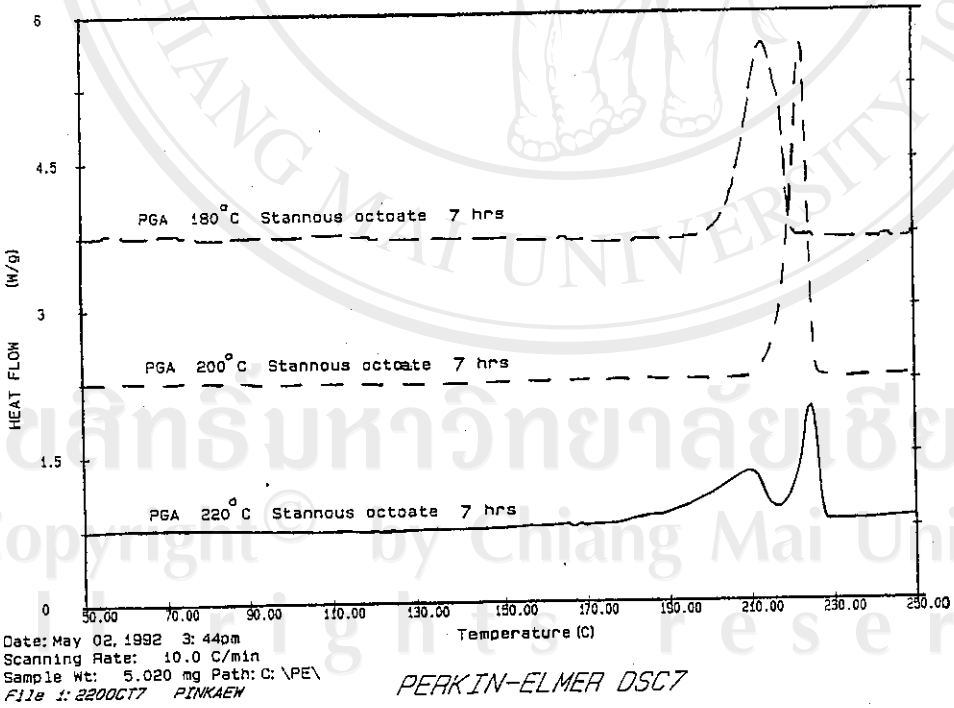

Fig. 3.17 : DSC curves of crude PGA initiated by stannous octoate showing the effect of reaction temperature.

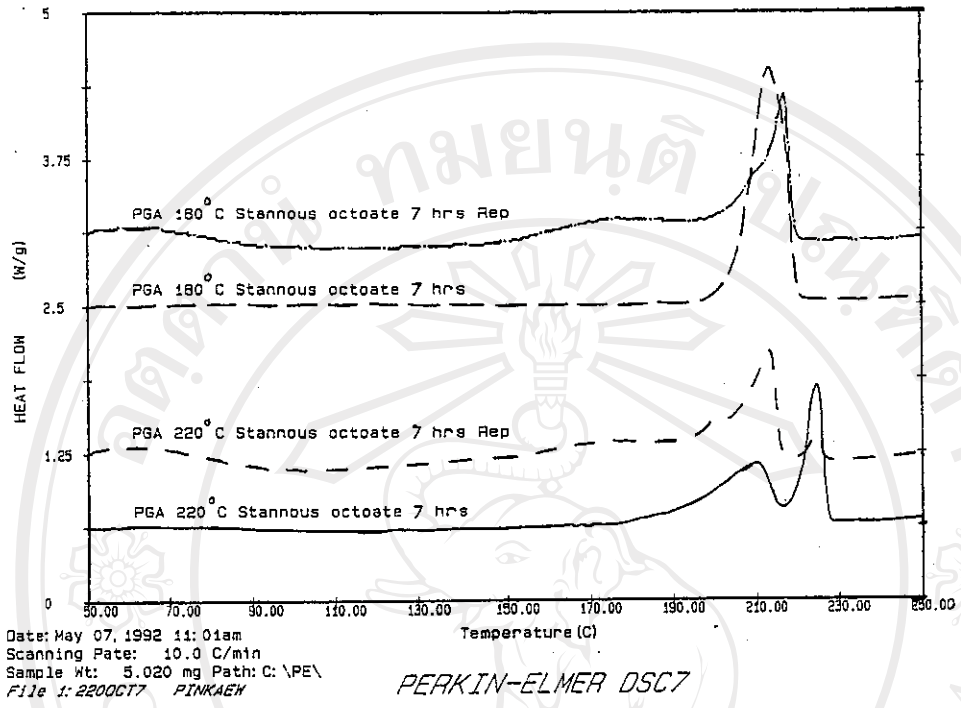

Fig. 3.18 : DSC curves of PGA initiated by stannous octoate showing the effect of purification by reprecipitation.

3.3.2.3.2 Discussion

From the results in Tables 3.13-3.15 and Figs. 3.16-3.18, similar conclusions can be drawn to those described in the previous two sections for $Al(C_2H_5)_3$ and SbF_3-initiation.

For example, increasing reaction time after solidification tends to have little effect other than that of annealing the sample, resulting in a more uniform size distribution of the crystalline regions. The molecular weight of the polymer appears to be "frozen-in" with little evidence of any continued solid-state polymerisation within the time-scale of the experiment.

The effect of increasing the polymerisation temperature from 180 °C to 200 °C is to increase and narrow the melting range (from DSC) until, at 220 °C, thermal degradation takes over. This sequence of events is clearly shown in Fig. 3.17 through the marked changes in the DSC melting peaks. Clearly, an optimum temperature exists at which the polymer molecular weight can attain its maximum value without accompanying thermal degradation. Molecular weights obtained here are again generally low ($[\eta] < 0.1$ dl/g) but this is probably due in part to the use of a higher initiator concentration (1% by mole of monomer) than is actually necessary in this reaction.

Again, purification of the crude PGA by reprecipitation from solution in hot DMSO as solvent had some opposite effects to those intended. Instead of obtaining a purer product, the reprecipitated PGA was contaminated with residual DMSO solvent which remained even after prolonged washing and vacuum drying at 90 °C. This effect is reflected in the DSC curves in Fig. 3.18.

In summary, stannous octoate is another suitable initiator for glycolide polymerisation. It has the advantages of being an

easily handled liquid, much less sensitive to air and moisture than $Al(C_2H_5)_3$, and does not require a "coinitiator" in order to be effective. The mechanism of stannous octoate-initiation will now be described.

Stannous octoate is generally considered to be an anionic-type initiator, acting via the mechainsm shown in Scheme 3.4 for the ring-opening polymerisation of glycolide. In this mechanism, nucleophilic attack of the initiating octoate anion occurs at the carbonyl-carbon of the monomer ring. The ring then opens in such a way as to form the more stable propagating anion [17-18, 44, 55].

Initation

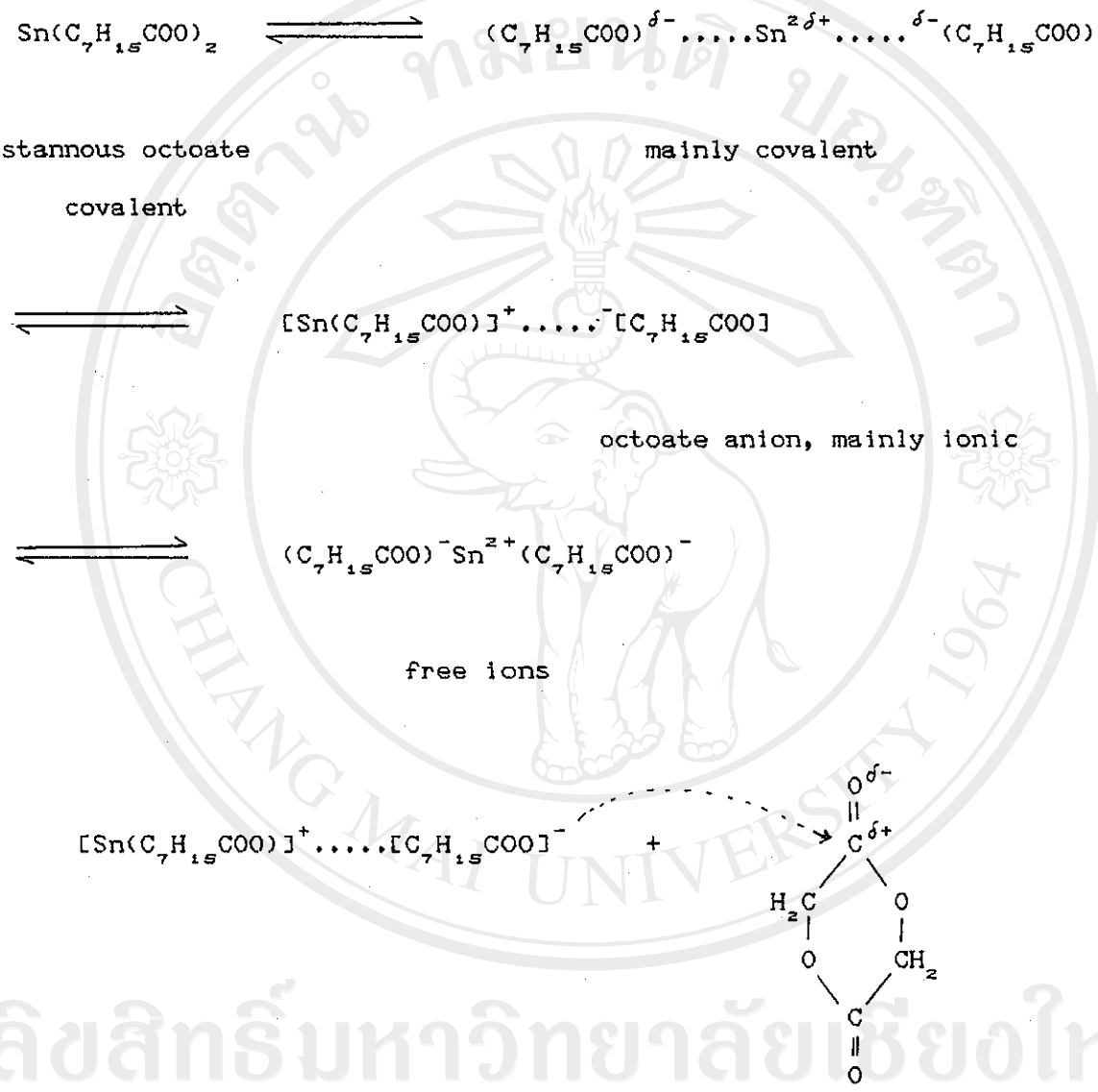

(...continued on next page)

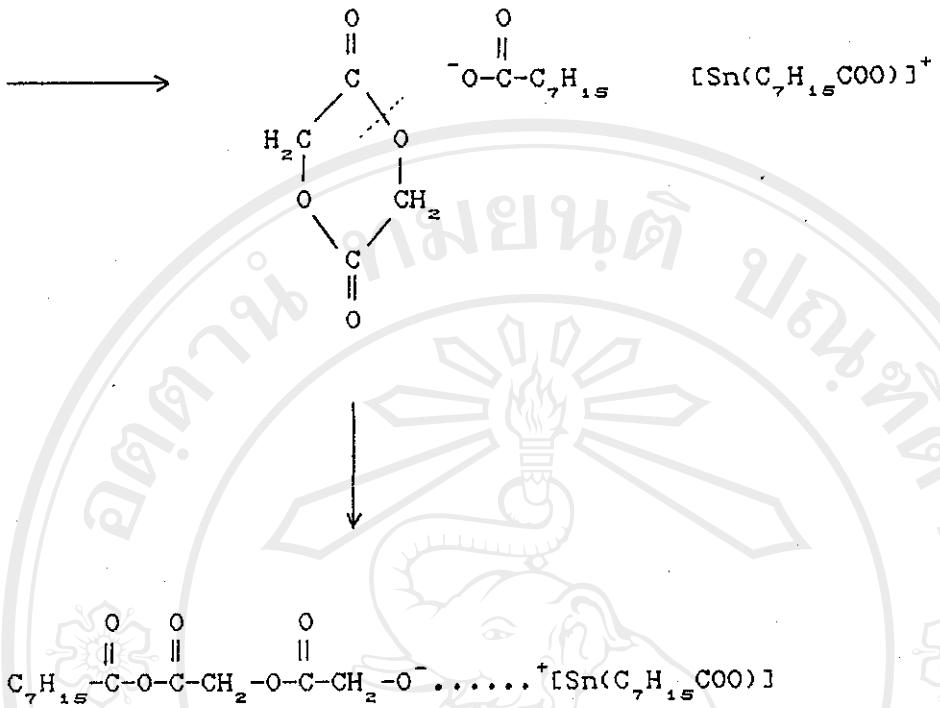

Propagation

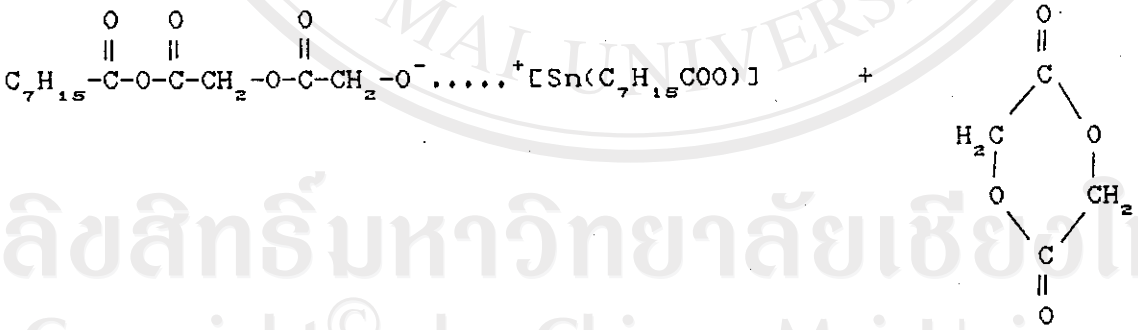

(...continued on next page)

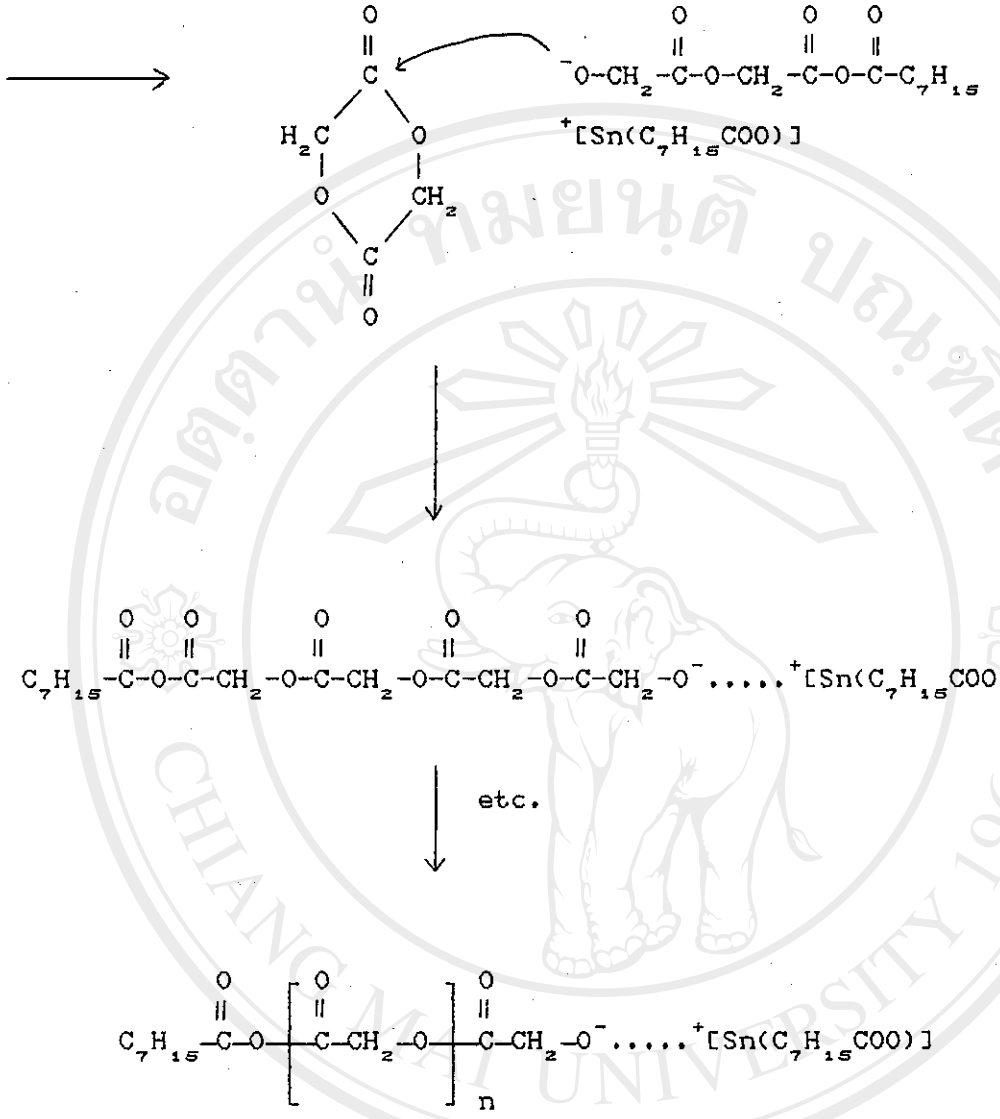

(...continued on next page)

Termination

(1) e.g., by chain transfer with adventitious moisture impurities

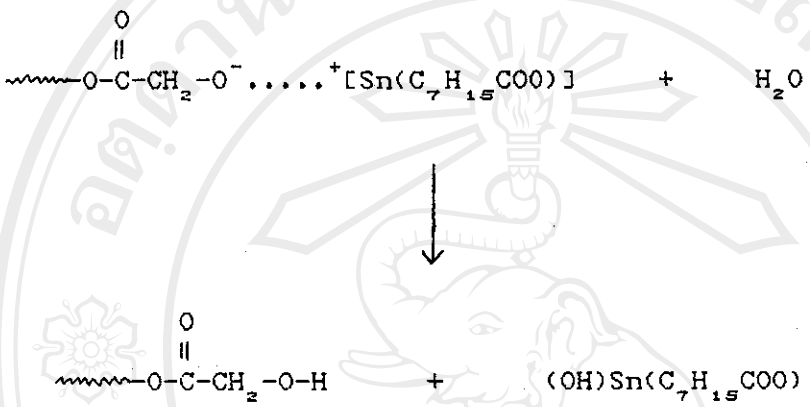

or (2) by re-association with counterion (lower probability)

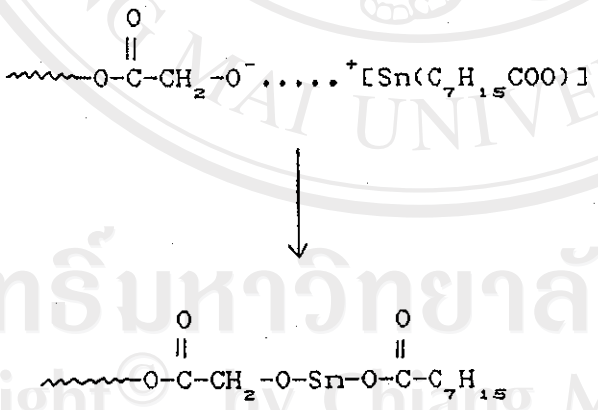

Scheme 3.4 : **Proposed mechanism for the stannous octoate initiated anionic ring-opening polymerisation of glycolide.**

It should be noted that in the initiation and subsequent steps, the active site at the end of the chain is accompanied by a counterion which can influence the reaction kinetically [70]. Propagation involves the successive insertion of monomer molecules (glycolide) into the terminal ionic bond of the growing chain, followed by nucleophilic attack of the anion on the monomer. This process of chain growth continues until all the monomer has been consumed, or until the reaction is terminated.

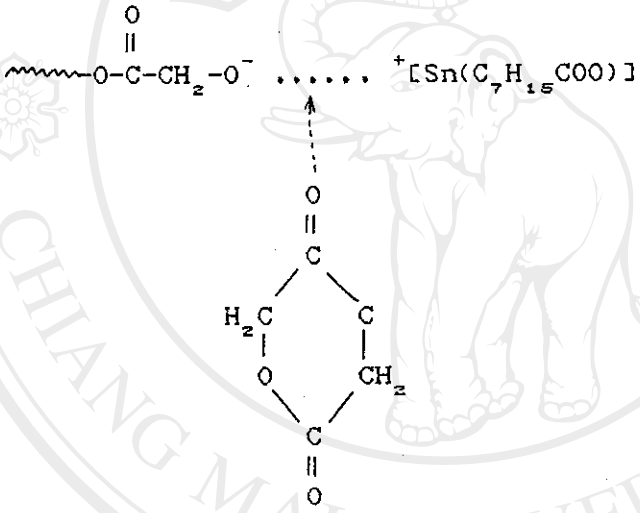

Termination of the chains occurs either accidentally or deliberately when the active chain end reacts with a molecule of water or other protonic reagent. However, it is important to note that, if termination reagents are absent, the chains could remain active indefinitely. Such nonterminated polymeric anions are referred to as "living polymers". In practice, however, it is impossible to remove all traces of water from the inside of glass equipment, even under high vacuum or in an inert atmosphere with rigorously cleaned reagents

and glassware. Any moisture present terminates the growing chain by proton transfer.

The hydroxide ion is usually not sufficiently nucleophilic to re-initiate polymerisation and so the kinetic chain is broken. Thus, "free" water has an especially negative effect on ionic polymerisations due to its activity as a chain transfer agent. The adventitious presence of other proton donors are not usually much of a problem [44].

3.3.2.4 Polymerisation using Stannous Oxalate as Initiator

The polymerisation procedure and conditions were the same as previously described in 3.3.2.1 except that 0.035 g of stannous oxalate were added as the initiator.

3.3.2.4.1 Polymer Characterisation

(A) Physical Characteristics

Table 3.16 describes the colours of the PGA products

obtained using stannous oxalate as initiator. The colours were generally lighter than those obtained using the previous initiators.

(B) Structural Analysis by Infrared Spectroscopy

The polymer IR spectra were similar to those shown previously. An example is given in Fig. 3.19 compared with that for the corresponding aluminium triethyl initiated product in Fig. 3.20.

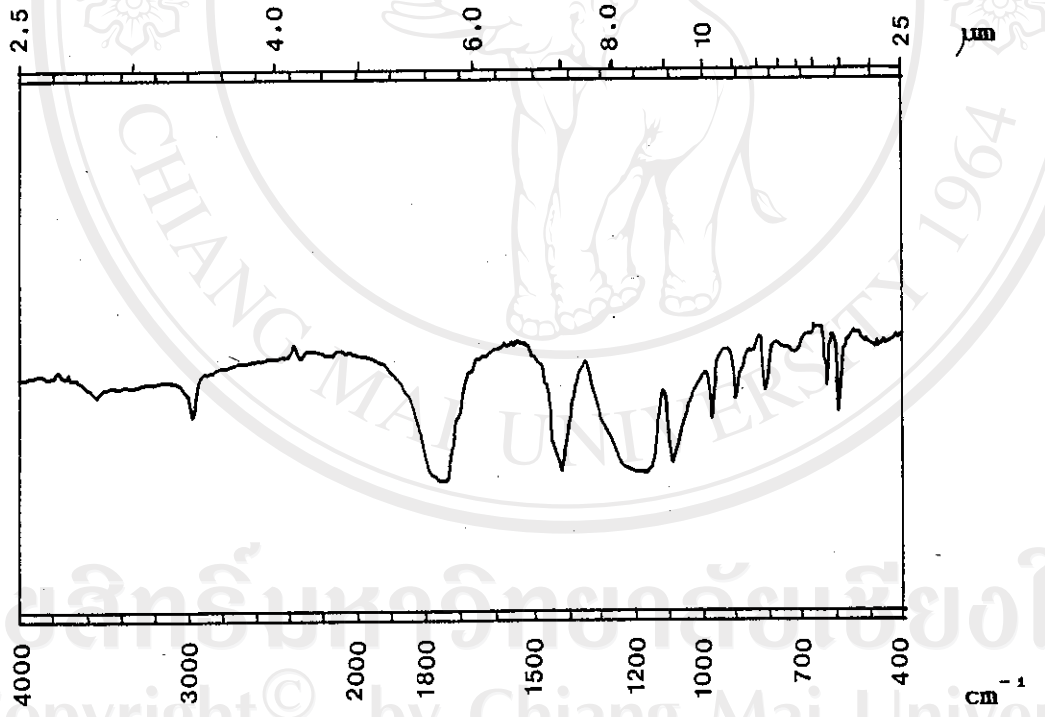

Fig. 3.19 : Infrared spectrum of crude PGA obtained using stannous oxalate as initiator at 200°C after 1 hour.

Table 3.16 : Variation in colour of the poly(glycolic acid) products obtained at different polymerisation times and temperatures using stannous oxalate as initiator.

Reaction Time (hrs)	180 °C		200 °C		220 °C	
	Crude PGA	Pure PGA	Crude PGA	Pure PGA	Crude PGA	Pure PGA
10 mins	pale cream	white	pale cream	white	pale cream	white
30 mins	"	"	"	"	"	pale cream
1	"	"	"	"	cream	"
2	"	"	cream	"	"	"
3	"	"	"	"	pale brown	"
4	cream	"	"	"	"	"
5	"	"	"	"	"	"
6	"	"	"	"	"	"
7	"	"	"	"	"	"

Note : all of the products were obtained in the form of solid powders after grinding and drying to constant weight in a vacuum oven at 90 °C.

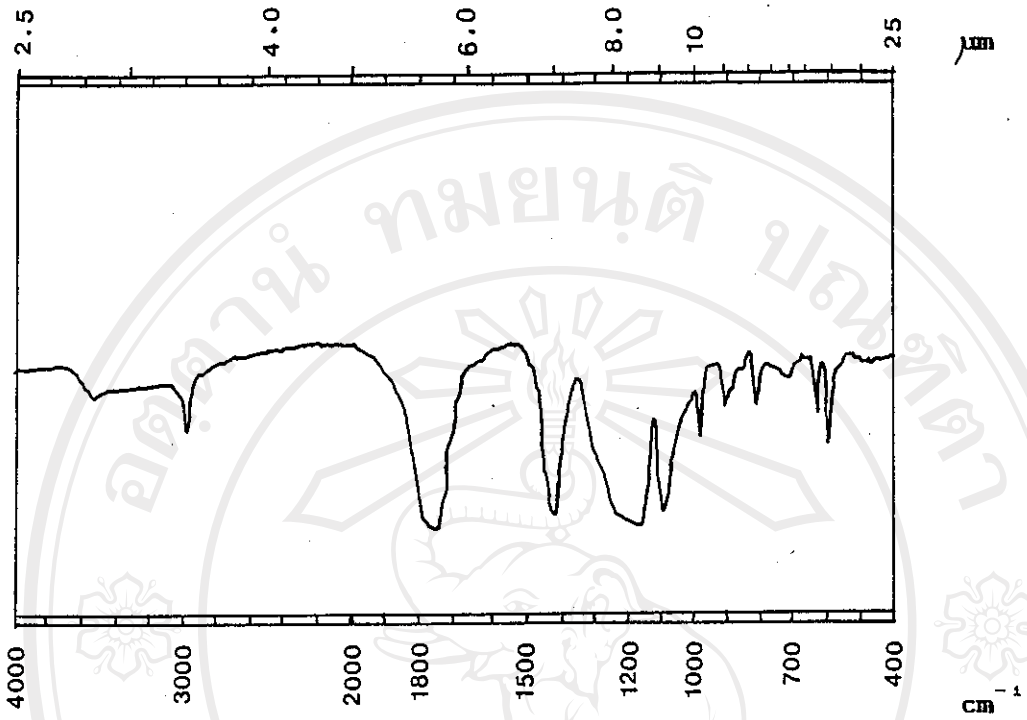

Fig. 3.20 : Infrared spectrum of crude PGA obained using aluminium triethyl as initiator at 200 °C after 1 hour.

(C) Melting Characteristics

The melting characteristics of the PGA products obtained via stannous oxalate initiation were studied and the results are presented in Tables 3.17-3.19.

(D) **% Crystallinity**

The heats of fusion and corresponding percent crystallinities obtained from DSC are also shown in Tables 3.17-3.19. The DSC curves are compared in Figs. 3.21-3.23.

(E) **Intrinsic Viscosity : Solomon-Ciuta One-Point Approximation Method**

The results of the determinations of the polymer intrinsic viscosities are also shown in Tables 3.17-3.19.

Table 3.17 : Physical characterisation for poly(glycolic acid) initiated by stannous oxalate at 180 °C.

Reaction Time (hrs)	MELTING POINT/RANGE, °C				CRYSTALLINITY				INTRINSIC VISCOSITY [η], dl/g
	from Buchi SMP-20		from DSC *		Crude PGA		Pure PGA		
	Crude	Pure	Crude	Pure	Heat of Fusion (J/g)	% Crystallinity	Heat of Fusion (J/g)	% Crystallinity	Pure PGA
10 mins	199-202	150-153							0.020
30 mins	197-200	152-155	187.68		30.46	16.1			0.055
1	195-200	150-153							0.030
2	200-204	150-152							
3	212-214	150-153							
4	214-216	150-152							0.030
5	213-216	159-162							
6	208-211	160-163							
7	205-208	161-164	215.88	217.78	107.38	56.7	130.80	69.0	0.034

* taken as temperature of melting peak max

Table 3.18 : Physical characterisation for poly(glycolic acid) initiated by stannous oxalate at 200 °C.

Reaction Time (hrs)	MELTING POINT/RANGE, °C				CRYSTALLINITY				INTRINSIC VISCOSITY [η], dl/g
	from Buchi SMP-20		from DSC *		Crude PGA		Pure PGA		
	Crude	Pure	Crude	Pure	Heat of Fusion (J/g)	% Crystallinity	Heat of Fusion (J/g)	% Crystallinity	Pure PGA
10 mins	210-214	194-196							0.123
30 mins	213-216	190-194	222.50		68.15	36.0			0.063
1	217-219	190-193							0.042
2	213-216	192-195							
3	213-216	191-195							
4	214-217	191-194							.046
5	215-218	192-195							
6	215-218	194-196							
7	215-218	195-197	221.89	216.79	106.54	56.2	122.71	64.8	0.059

* taken as temperature of melting peak maximum

Table 3.19 : Physical characterisation for poly(glycolic acid) initiated by stannous oxalate at 220 °C.

Reaction Time (hrs)	MELTING POINT/RANGE, °C				CRYSTALLINITY				INTRINSIC VISCOSITY [η], dl/g
	from Buchi SMP-20		from DSC *		Crude PGA		Pure PGA		
	Crude	Pure	Crude	Pure	Heat of Fusion (J/g)	% Crystallinity	Heat of Fusion (J/g)	% Crystallinity	Pure PGA
10 mins	193-195	190-193							0.040
30 mins	210-214	189-192	217.46		67.76	35.8			0.018
1	210-215	183-186							0.040
2	211-216	177-180							
3	209-213	170-173							
4	207-210	170-173							0.040
5	209-215	180-183							
6	210-213	180-182							
7	210-213	180-183	214.65	219.35	84.98	44.8	141.96	74.9	0.042

* taken as temperature of melting peak maximum

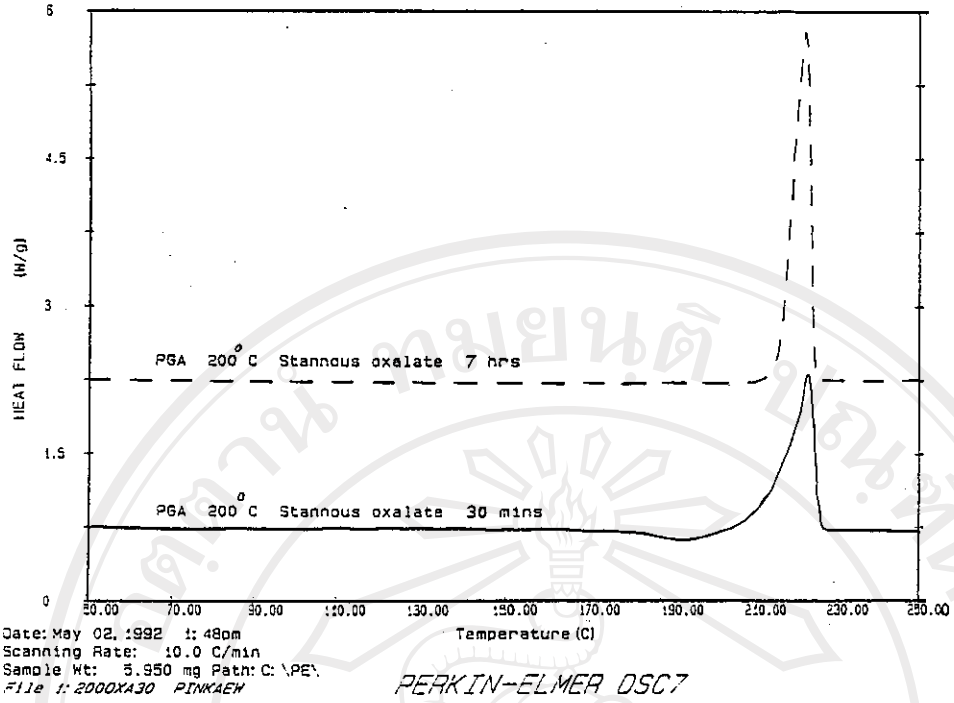

Fig. 3.21 : DSC curves of crude PGA initiated by stannous oxalate showing the effect of reaction time.

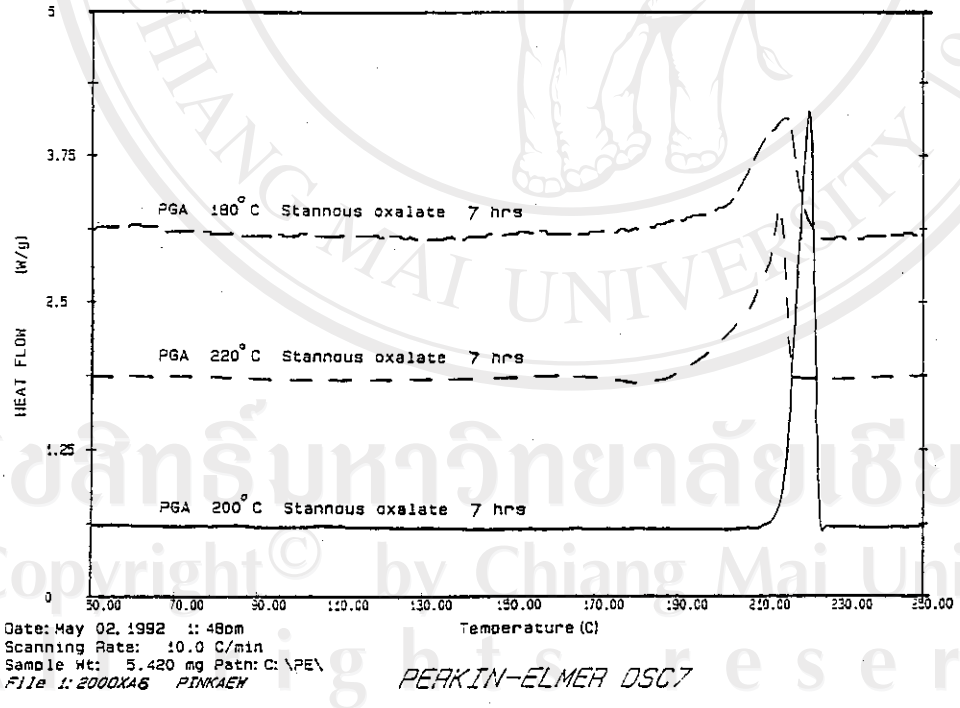

Fig. 3.22 : DSC curves of crude PGA initiated by stannous oxalate showing the effect of reaction temperature.

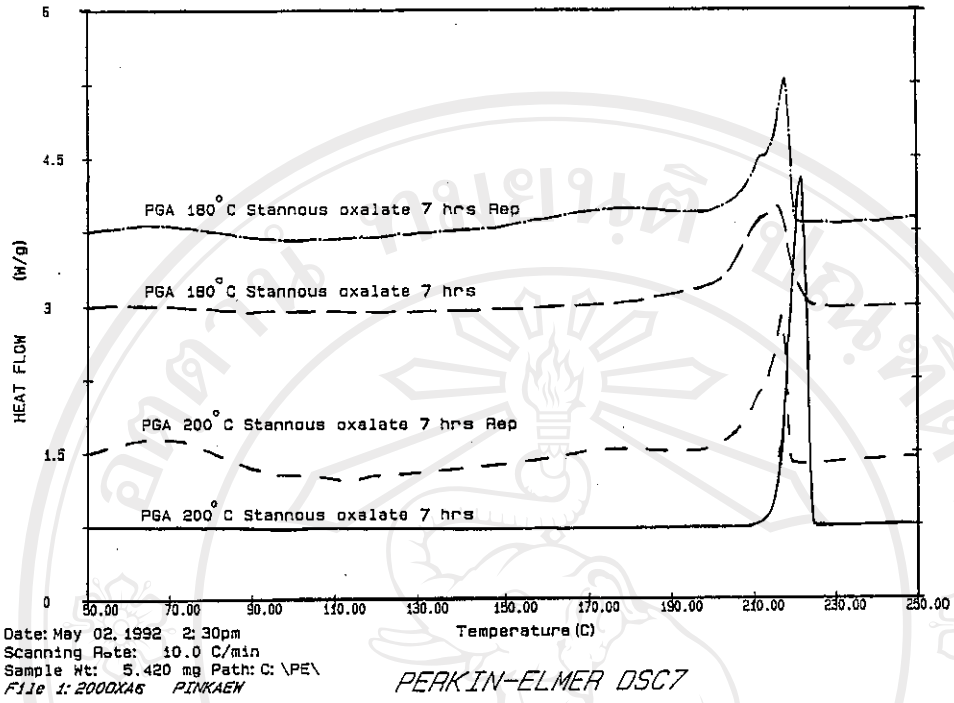

Fig. 3.23 : DSC curves of PGA initiated by stannous oxalate showing the effect of purification by reprecipitation.

3.3.2.4.2 Discussion

As might be expected, the results shown in Tables 3.17-3.19 and Figs. 3.21-3.23 for stannous oxalate exhibit similar tends to those observed previously for stannous octoate. Again the optimum temperature for polymerisation appears to be 200 °C, as indicated by the DSC curves in Fig. 3.22. At this temperature, the polymerisate solidified after about 1 hour. Continued heating (annealing) for up

to 7 hours again provided evidence of further crystallisation in the solid-state towards an equilibrium morphology (Fig. 3.21). Polymer molecular weights were again low ([n] < 0.1 dlg^{-1}) although this can probably be improved upon in future work by reducing the initiator concentration below the 1 mole % (based on glycolide monomer) used in this project.

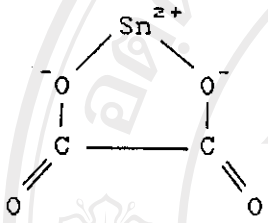

stannous oxalate

$(C_7H_{15}COO)Sn(OOCC_7H_{15})$

stannous octoate

The similarities between the PGA products obtained at the optimum temperature of 200 °C from stannous oxalate and stannous octoate initiation suggest that the exact nature of the ester group does not have a particularly important effect on the initiating efficiency of the resulting anion. The polymerisation mechanisms can therefore be assumed to be similar, as described for stannous octoate in the preceding section. The only difference is in the nature of the initiation step since the oxalate group is a single dianion whereas the octoate groups in stannous octoate are separate monoanions. A notable consequence of this is that the counterion in the stannous oxalate mechanism cannot exert the same influence on the propagating chain end [17-18, 44].

Initiation

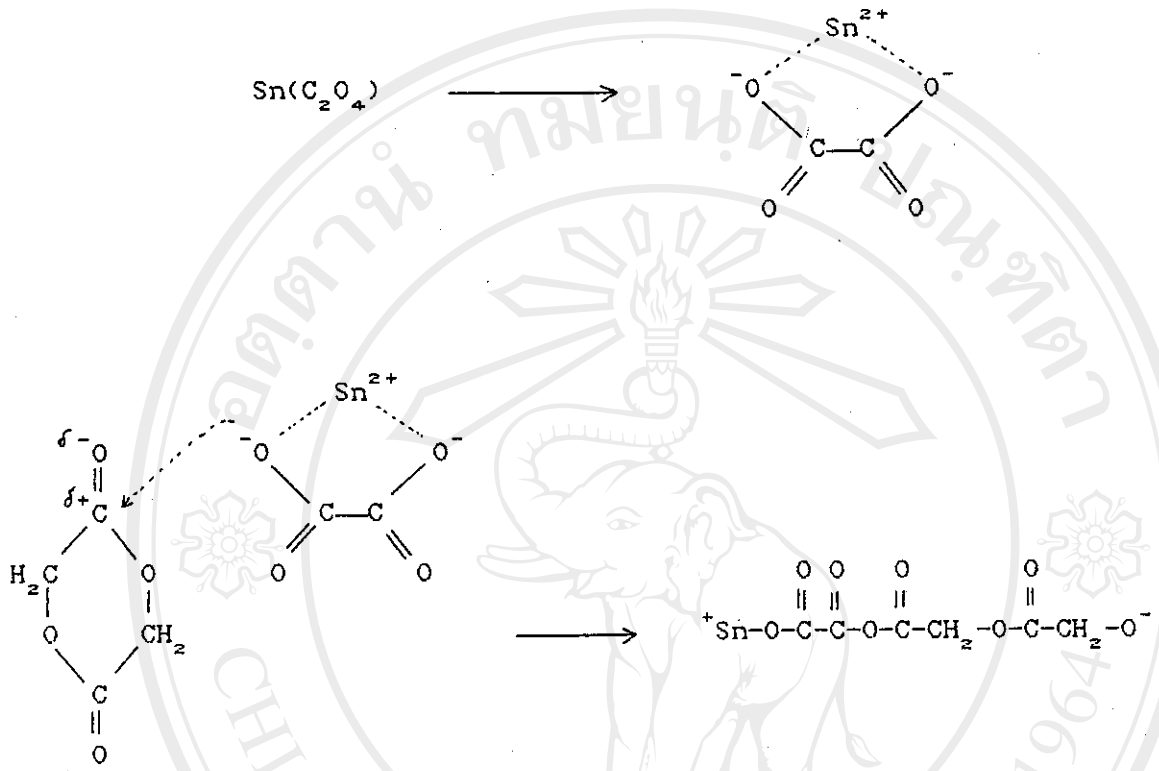

Propagation

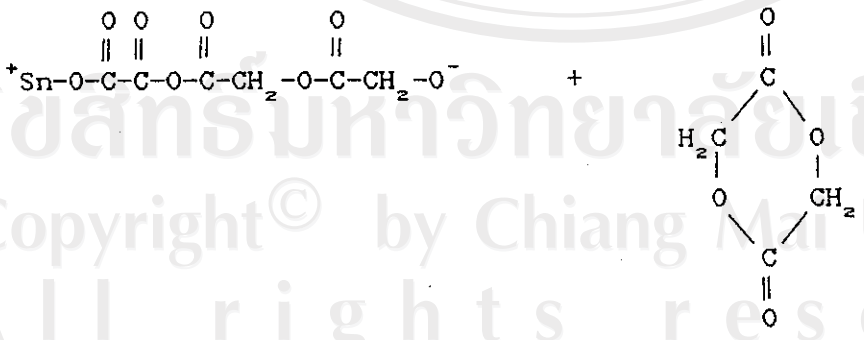

(...continued on next page)

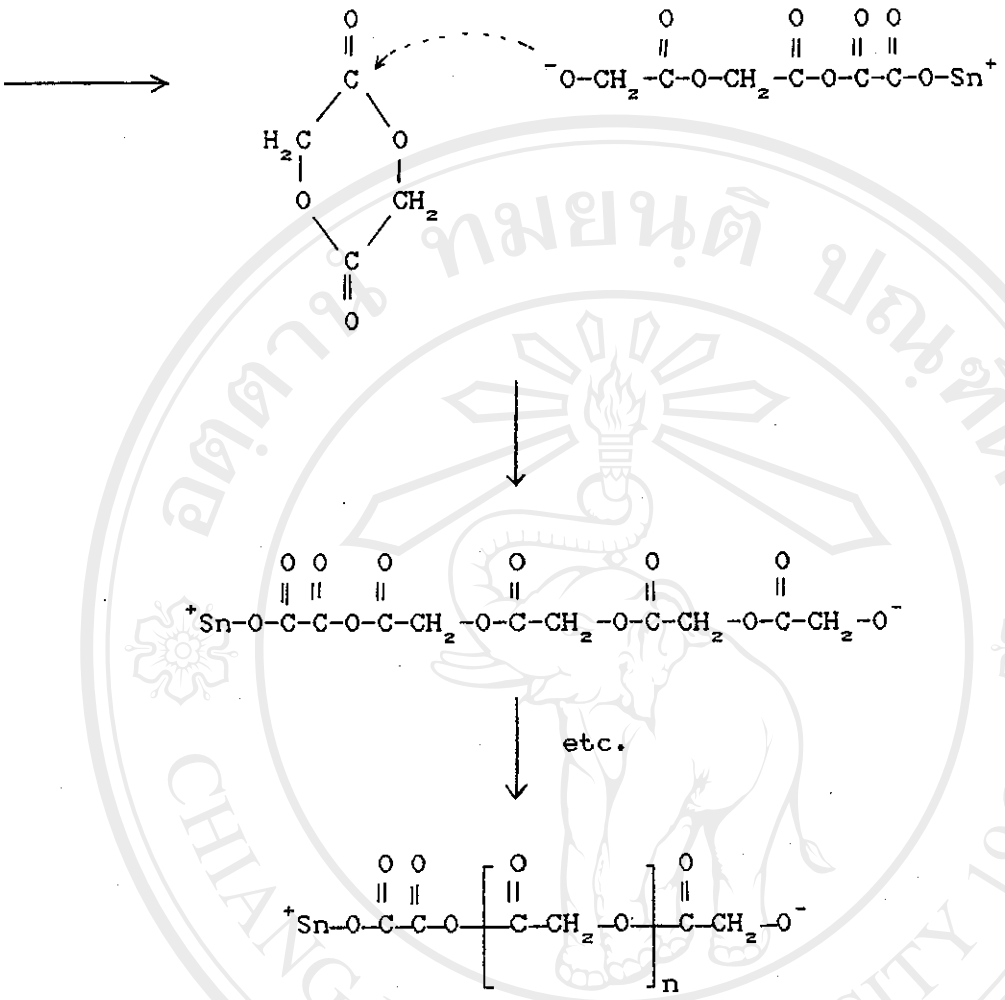

Termination (e.g., by chain transfer to adventitious moisture impurities)

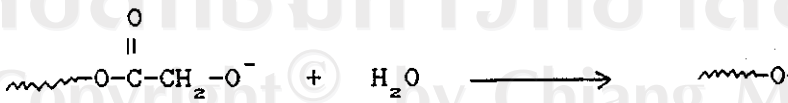

Scheme 3.5 : Proposed mechanism for the stannous oxalate initiated anionic ring-opening polymerisation of glycolide.

Comparison of Initiators

The four polymerisation initiators used in this work are compared in Figs. 3.24-3.26 at each of the three temperatures studied. On comparing the DSC curves, the following inferences can be drawn :

(1) Under the same reaction conditions (temperature, time,etc.) and at the same initiator concentration (1 mole %), the different initiators produce different results. This is obviously related to their different reactivities towards the glycolide ring, a common feature in ring-opening polymerisation.

(2) Initiator efficiency is often judged in terms of high molecular weight and uniform matrix morphology of the polymer product. This is reflected to a large extent in the DSC curve as a high melting range over a narrow range of temperature. On this basis, aluminium triethyl would be judged as the best initiator at 180 °C (Fig. 3.24) and antimony trifluoride at 200 °C (Fig. 3.25). However, the differences at 180 °C and 200 °C are relatively small and, indeed, all four initiators can be considered as being suitable for glycolide polymerisation. At 220 °C, thermal degradation of the polymer occurs (Fig. 3.26) which is a function of the polymer rather than the initiator.

(3) Of these four initiators, aluminium triethyl has the disadvantage of being the most difficult to use. It is a hazardous, air- and

moisture-sensitive compound which requires careful handling in a controlled atmosphere (dry, O_2-free) glove box. It also needs to be prepared in solution which means that the crude polymer may contain trace amounts of solvent as a residual impurity. In contrast to this, the other three initiators can all be handled easily without any special precautions and can be mixed directly with the monomer in neat form.

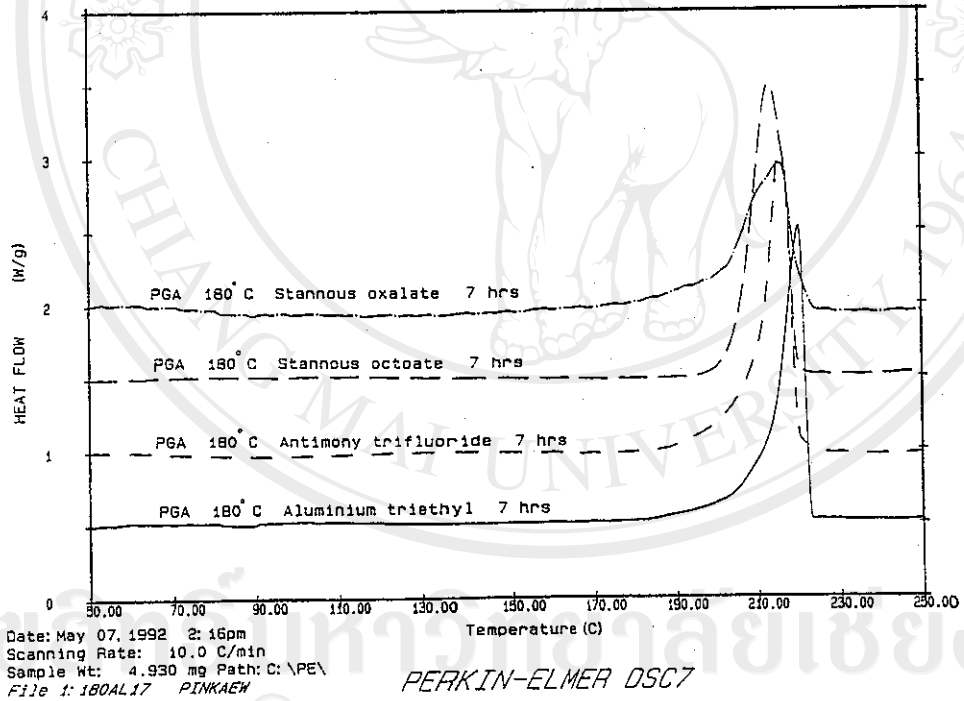

Fig. 3.24 : DSC curves of PGA showing the effect of varying the initiator at 180 °C.

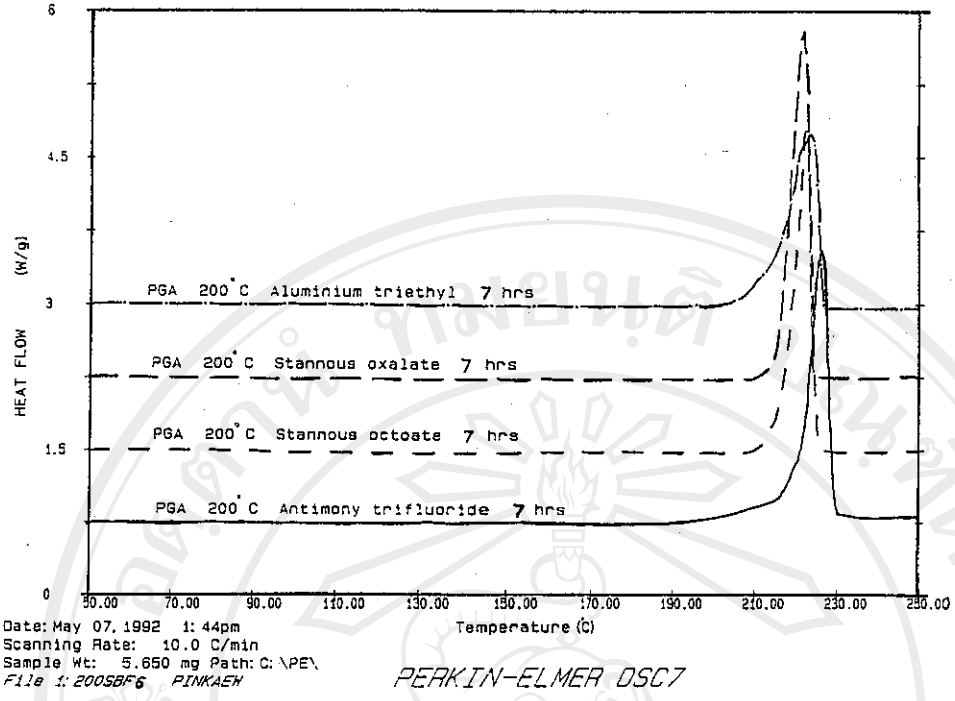

Fig. 3.25 : DSC curves of PGA showing the effect of varying the initiator at 200 °C.

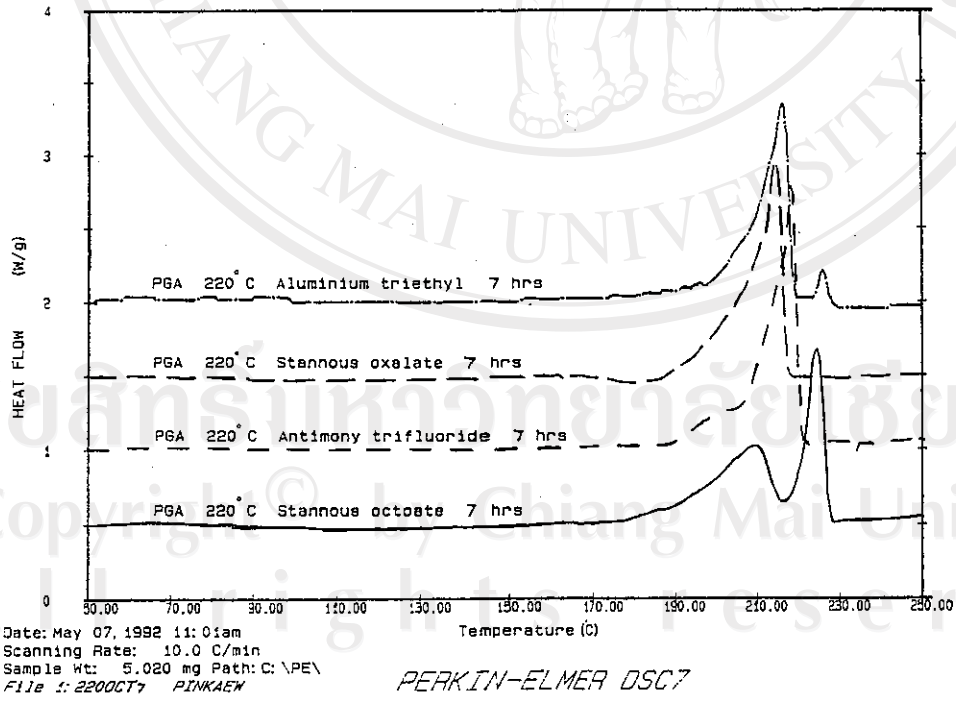

Fig. 3.26 : DSC curves of PGA showing the effect of varying the initiator at 220 °C.